research articles Journal of proteome research

Identification of Predictive Biomarkers for Response to Trastuzumab Using Plasma FUCA Activity and N-Glycan Identified by MALDI-TOF-MS

Kazuko Matsumoto,[†,§,#] Chikako Shimizu,[‡,#] Tokuzo Arao,[†] Masashi Andoh,[‡] Noriyuki Katsumata,[‡] Tsutomu Kohno,[‡] Kan Yonemori,[‡] Fumiaki Koizumi,[∥] Hideyuki Yokote,[†] Kenjiro Aogi,[⊥] Kenji Tamura,[‡] Kazuto Nishio,[*,†] and Yasuhiro Fujiwara[‡]

Department of Genome Biology, Kinki University School of Medicine, Osaka, Japan, Medical Oncology, National Cancer Center Hospital, Tokyo, Japan, First Department of Internal Medicine, Osaka Medical College, Osaka, Japan, Shien Lab, National Cancer Center Hospital, Tokyo, Japan, and Department of Surgery, National Hospital Organization Shikoku Cancer Center, Matsuyama, Japan

Received August 19, 2008

The aim of this study was to identify glycobiological biomarkers that indicate sensitivity to trastuzumab, a humanized monoclonal antibody against HER2 in plasma samples from breast cancer patients. Plasma samples were obtained from 24 breast cancer patients treated with trastuzumab monotherapy. The catalytic activities of plasma α1-6, fucosyltransferase (FUT8) and α-L fucosidase (FUCA) were analyzed using high-performance liquid chromatography (HPLC) and spectrophotometer, respectively. The plasma N-glycan profiles were investigated using matrix-assisted laser desorption/ionization time-of-flight mass spectrometry (MALDI-TOF-MS). Plasma FUT8 activity was not significantly correlated with either the clinical response or progression-free survival (PFS). On the other hand, plasma FUCA activity was significantly correlated with PFS ($p < 0.05$). The MALDI-TOF-MS analysis of the plasma N-glycan profile revealed that the expression of 2534 *m/z* N-glycan was lower in patients with progressive disease (PD) and was correlated with PFS. Low expression of 2534 *m/z* N-glycan discriminated between PD and non-PD with 75% sensitivity and 82% specificity. We demonstrated that the plasma FUCA activity and 2534 *m/z* N-glycan may be predictive biomarkers of sensitivity to trastuzumab. Our results suggest that glycosylation analysis may provide useful information for determining clinical cancer therapy and provide novel insight into biomarker studies using glycobiological tools in the field of breast cancer.

Keywords: FUT8 • FUCA • N-glycan • trastuzumab • breast cancer

Introduction

The glycosylation of proteins is an important post-translational modification that plays a critical role in cancer biology including cellular growth, differentiation, adhesion and metastasis.[1-4] Specific carbohydrate chains and glycosyltransferase are associated with the biological functions of cancer cells.[5,6] Recently, many researchers have evaluated the use of glycosylated proteins, such as carbohydrate antigens CA19−9 and CA125, as biomarkers for early diagnosis or tumor progression.[7-9]

The fucosylation of N-linked oligosaccharides is one of the most important glycosylation events in biological function, including cancer.[10,11] For example, fucosylated α-fetoprotein is a highly specific tumor marker of hepatocellular carcinoma.[12] α1-6, Fucosyltransferase (FUT8) is known to transfer a fucose residue to N-linked oligosaccharides on glycoproteins.[13] A series of studies have demonstrated that nonfucosylated antibody, which is produced by the knockout of the FUT8 gene, enhances antibody-dependent cellular cytotoxicity (ADCC) and the cytotoxic effect of the antibody.[14-16] These results indicate that FUT8 plays an important role in ADCC activity. α-L fucosidase (FUCA), on the other hand, is a lysosomal hydrolase that has been identified in tissues and serum. Serum FUCA activity is reportedly correlated with early detection in hepatocellular carcinoma[17] and may be a useful prognostic marker and a predictive marker of tumor recurrence in colorectal cancer.[18,19]

HER2 (also known as NEU, EGFR2, or ERBB2) is a member of the epidermal growth factor receptor (EGFR) family. HER2 is amplified in 25−30% of human primary breast cancers and predicts a poor prognosis.[20-22] Trastuzumab (Herceptin; Roche, Basel, Switzerland), a humanized monoclonal antibody against HER2, is a potent anticancer agent that is used in standard chemotherapy against HER2-overexpressing breast cancer in

* To whom correspondence should be addressed. Kazuto Nishio, Department of Genome Biology, Kinki University School of Medicine, 377-2 Ohno-Higashi, Osaka-Sayama, Osaka, Japan. Tel: +81-72-366-0221. Fax: +81-72-366-0206. E-mail: knishio@med.kindai.ac.jp.

† Kinki University School of Medicine.

‡ Osaka Medical College.

§ Medical Oncology, National Cancer Center Hospital.

# These authors contributed equally to this work.

∥ Shien Lab, National Cancer Center Hospital.

⊥ National Hospital Organization Shikoku Cancer Center.

10.1021/pr800655p CCC: $40.75

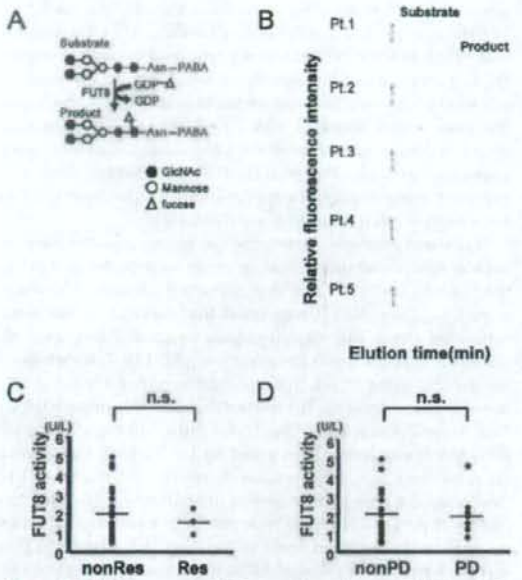

Figure 1. (A) Schema of α1-6, fucosyltransferase (FUT8) reaction used to measure FUT8 enzymatic activity. Asn, asparagine; PABA, 4-(2-pyridylamino) butylamine. (B) HPLC data for plasma FUT8 activities in clinical samples. The substrate (GnGn-bi-Asn-PABA) is fucosylated by FUT8 and detected as the product. FUT8 activity is measured using HPLC. The enzyme activities were analyzed in duplicate. (C) Plasma FUT8 activity and clinical response. Res, responder group (complete response + partial response); non-Res, nonresponder group (stable disease + progressive disease). n.s.: not significant. (D) Plasma FUT8 activity and clinical response. PD, progressive disease group; nonPD, nonprogressive disease group. n.s.: not significant.

combination with other chemotherapeutic agents.[23,24] In some patients with HER2 overexpression, however, trastuzumab dose not have any anticancer effect. In addition, trastuzumab can induce severe adverse effects, such as cardiac dysfunction.

Therefore, biomarkers are needed to predict the clinical outcome of trastuzumab therapy in patients with breast cancer. We previously reported that trastuzumab-induced ADCC is a major mechanism of action,[25] in addition to the effects of anti-EGFR antibody.[26] We have also identified a sensitivity determinant factor for EGFR-targeting drugs[27,28] and recently demonstrated that FUT8 regulated the fucosylation level of EGFR and modifies EGF-mediated cellular growth and sensitivity to EGFR tyrosine kinase inhibitor.[29]

In the present study, we attempted to identify predictive biomarkers of sensitivity to trastuzumab, focusing on fucosylation and glycosylation. For this purpose, plasma FUT8 and FUCA activity and the N-glycan profiles were examined in breast cancer patients treated with trastuzumab monotherapy.

Materials and Methods

Patients and Blood Samples. This prospective study was started in August 2005 and enrollment at the National Cancer Center Hospital and Shikoku Cancer Center Hospital was completed in August 2007. Eligible patients had histologically confirmed, nonlife-threating, postoperative recurrent or stage IV HER2-positive breast cancer, and were intended to receive trastuzumab monotherapy. The HER2 status was confirmed using immunohistochemistry (IHC) 3+ or fluorescence in situ hybridization (FISH)-positive utilizing core needle biopsy (CNB) samples of the tumor tissue. All the patients were treated with trastuzumab (4 mg/kg on day 1 and thereafter at a dose of 2 mg/kg weekly), and 24 patients were evaluated. The response to trastuzumab therapy was evaluated based on a CT scan, magnetic resonance imaging (MRI) or ultrasound examination of the tumor before and 8 weeks after treatment and was classified according to the Response Evaluation Criteria in Solid Tumors. Plasma samples were obtained immediately before trastuzumab treatment, centrifuged and stored at −80 °C. The study was approved by the Institutional Review Boards of the National Cancer Center Hospital, Kinki University Hospital and Shikoku Cancer Center Hospital, and written informed consent was obtained from all the patients.

Table 1. Clinical Characteristics of Study Population[a]

characteristics		no. of patients	%
Age	Mean	60	
	Range	28–76	
Prior chemotherapy	Present	17	71
	Absent	6	25
	ND	1	4
Prior radiotherapy	Present	14	58
	Absent	9	38
	ND	1	4
PS	0	8	33
	1	15	63
	2	1	4
Metastasis	Lung	15	63
	Liver	3	13
	Bone	5	21
	Brain	2	8
	LN	10	42
	Others	2	8
Hormone receptor	ER (+)	12	50
	ER (−)	12	50
	PgR (+)	11	46
	PgR (−)	12	50
	ND	1	4

[a] ND, not determined; PS, performance status; ER, estrogen receptor; PgR, progesterone receptor.

FUT8 Activity Assay. The method used to perform the FUT8 activity assay has been previously described.[30] Briefly, the fluorescent substrate (GnGn-bi-Asn-PABA, Figure 1A) was purchased from Peptide Institute, Inc. (Osaka, Japan). The standard mixture for measuring FUT8 activity contained 50 μM of substrate, 200 mM of MES (pH 7.0), 1% Triton X, 500 μM of GDP-Fucose and 23 μL of the plasma sample in a final volume of 50 μL. The reaction mixture was incubated at 37 °C for 6 h, and the reaction was stopped by heating at 100 °C for 1 min. The sample was then centrifuged at 15 000*g* for 10 min, and the supernatant (5 μL) was used for the analysis. The product was separated using high-performance liquid chromatography (HPLC) with a TSK-gel ODS-80TM column (4.6 × 150 mm). Elution was performed at 55 °C with a 20 mM acetate buffer, pH 4.0, containing 0.1% butanol. The fluorescence of the column elute was detected using a fluorescence photometer (HITACHI Fluorescence Spectrophotometer 650−10LC). The excitation and emission wavelengths were observed at 320 and 400 nm, respectively. The product area was used to calculate the enzyme activity (U/L) in all the patients. The enzyme activities were analyzed in duplicate.

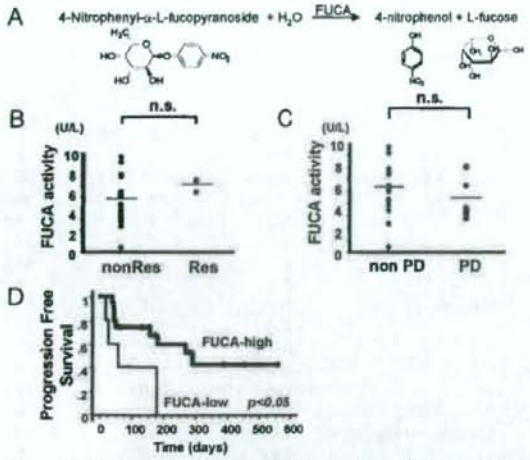

Figure 2. (A) Reaction pathway of α-L fucosidase (FUCA) activity. The substrate (4-nitrophenyl-α-L-fucopyranoside) is defucosylated by FUCA and the products are detected. FUCA activity is measured using spectrophotometer. The enzyme activities were analyzed in duplicate. (B) Plasma FUCA activity and clinical response. Res, responder group (complete response + partial response); nonRes, nonresponder group (stable disease + progressive disease). n.s.: not significant. (C) Plasma FUCA activity and clinical response. PD, progressive disease group; nonPD, nonprogressive disease group. n.s.: not significant. (D) Kaplan–Meier curve for progression-free survival (PFS) of trastuzumab treatment. Patients with a high plasma FUCA activity (4.3 > U/L) exhibited a significantly prolonged PFS ($p < 0.05$).

FUCA Activity Assay. The standard mixture for measuring α-L fucosidase activity contained 20 μL of the plasma sample, 2 mM of 4-nitrophenyl-α-L-fucopyranoside (Sigma, St. Louis, MO), and 50 mM of citrate buffer (pH 4.5) in a final volume of 150 μl. in a 96-well microplate. The mixture was incubated at 37 °C for 3 h, and the reaction was stopped by the addition of 100 μL of 0.4 M borate buffer (pH 9.8). The optical density was measured at 405 nm. One unit of enzyme was defined as the amount of enzyme required to produce 1 mmol of product per minute at 37 °C. The enzyme activities were analyzed in duplicate.

Purification of Plasma N-Glycan. Twenty-seven microliters of plasma sample was dissolved in 83 mM ammonium bicarbonate and 10 mM DL-dithiothreitol (Sigma-Aldrich, St. Louis, MO) in a final volume of 60 μL. The mixture was incubated at 60 °C for 30 min, and 10 μL of 123 mM iodoacetamide (Wako Pure Chemicals Co., Tokyo, Japan) was added. After incubation for 1 h at room temperature in the dark, 400 units of trypsin (Sigma-Aldrich) was added to the mixture. The mixture was incubated at 37 °C for 2 h, and the reaction was stopped by heating at 90 °C for 5 min. Five units of peptide *N*-glycosidase F (Roche Diagnostics, Mannheim, Germany) was added, and the mixture was incubated at 37 °C overnight. The internal standard (mannononaose-di-(*N*-acetyl-D-glucosamine), Sigma-Aldrich) was added, and N-glycan was purified from the mixture using BlotGlyco (Sumitomo Bakelite, Co., Tokyo, Japan) according to the manufacture's protocol.[31]

Mass Spectrometry Analysis. The purified samples were concentrated, and 0.5 μl. of the sample solution was applied to a sample plate target, then mixed with 0.5 μl. of the matrix solution. 2, 5-Dihydroxybenzoic acid (Aldrich) was dissolved in 50% acetonitrile using the matrix solution. After the samples had dried, MALDI-TOF-MS was performed using a Voyager-DE STR Workstation (Applied Biosystems) in reflector, positive ion mode. The number of laser shots was 300 × 2 shots and the mass range acquired was 700–5000 Da. The N-glycan structure was achieved using the GlycoSuite online database, proteome System. The MALDI-TOF-MS spectra data was exported using Voyager Biospectrometry Workstation ver 5.1, Data Explorer Software (Applied Biosystem).

Statistical Analysis. The statistical analyses of the enzyme activity assays and the clinical outcome were performed using the Student's *t*-test by StatView version 5 software (SAS Institute, Inc., Cary, NC). Progression-free survival curves were estimated using the Kaplan–Meier method (StatView). All plasma N-glycans peaks obtained from MALDI-TOF-MS were normalized using an internal standard (mannononaose-di-(*N*-acetyl-D-glucosamine)). The normalized data was imported into BRB Array Tools software ver. 3.3.0 (http://linus.nci.nih.gov/BRB-ArrayTools.html), developed by Dr. Richard Simon and Dr. Amy Peng. N-Glycan peaks were selected for analysis if the peak was observed in over 50% of the patients (> 12 patients); finally, 31 peaks of N-glycan were selected. A statistical analysis comparing the N-glycan peaks to response to treatment or PFS was performed. A p-value of < 0.05 was considered significant.

Result

Patient Characteristics. Twenty-four patients were evaluated in this study. The mean patient age was 60 years (range 28–76 years). Seventy-one percent (17/24 pts) of the patients had received prior adjuvant chemotherapy, and 58% (14/24 pts) of the patients had received prior radiotherapy. Almost all the patients had a performance status (PS) of 0 or 1 (23/24 pts), and the metastatic sites and hormone receptor status were shown (Table 1). Table 1 summarizes the clinical features of the patients.

Plasma FUT8 Activity and Clinical Outcome. Plasma FUT8 activity was measured using reverse-phase HPLC with a fluorescent substrate (Figure 1A). A representative elution pattern of FUT8 activity in the plasma sample is shown in Figure 1B. The elution times of the substrate and product were 15 and 27 min, respectively. The product area was calculated to determined the overall catalytic activity. The average FUT8 enzyme activity was 2.0 ± 1.3 U/L (average ± SD; range, 0.5 to 5.0 U/L). Regarding the clinical outcome, the FUT8 catalytic activities of responders (CR, complete response; PR, partial response, $n = 3$) and nonresponders (SD, stable disease; PD, progressive disease, $n = 21$) were 1.6 ± 0.7 U/L and 2.0 ± 1.4 U/L, respectively. The activities of the PD and non-PD groups were 1.9 ± 1.2 U/L and 2.0 ± 1.4 U/L, respectivily. No significant correlations between FUT8 activity and the clinical response to trastuzumab were seen (Figure 1C,D). Also, no significant correlations were seen between FUT8 activity and progression-free survival (PFS, data not shown). These results suggest that plasma FUT8 activity is not a useful biomarker for this population.

Correlation of Plasma FUCA Activity and PFS. Plasma FUCA activity was examined using spectrophotometer and 4-nitrophenyl-α-L-fucopyranoside (Figure 2A). The average FUCA enzyme activity was 6.1 ± 2.1 U/L (average ± SD; range, 1.5 to 9.7 U/L). The activities of responders, nonresponders, the PD group and the non-PD group were 7.2 ± 0.6, 5.9 ± 2.2, 5.5 ± 1.8 and 6.3 ± 2.2 U/L, respectively. No significant correlations between FUCA activity and the clinical response to trastuzumab

Table 2. List of Predominant Oligosaccharides in Patient Serum Samples[a]

measured MS (m/z)	putative structure
1286.6	ND
1300.6	(Hex)2 (HexNAc)2 (Deoxyhexose)2
1495.5	(Hex)2 + (Man)3(GlcNAc)2
1657.6	(Hex)3 + (Man)3(GlcNAc)2
1701.6	ND
1723.7	(HexNAc)2 (Deoxyhexose)1 + (Man)3(GlcNAc)2
1739.7	(Hex)1 (HexNAc)2 + (Man)3(GlcNAc)2
1841.7	(Hex)1 (HexNAc)1 (NeuAc)1 + (Man)3(GlcNAc)2
1885.7	(Hex)1 (HexNAc)2 (Deoxyhexose)1 + (Man)3(GlcNAc)2
1901.7	(Hex)2 (HexNAc)2 + (Man)3(GlcNAc)2
1926.7	(HexNAc)3 (Deoxyhexose)1 + (Man)3(GlcNAc)2
2047.8	(Hex)2 (HexNAc)2 (Deoxyhexose)1 + (Man)3(GlcNAc)2
2088.8	(Hex)1 (HexNAc)3 (Deoxyhexose)1 + (Man)3(GlcNAc)2
2121.8	(Hex)1 (HexNAc)1 (Deoxyhexose)4 + (Man)3(GlcNAc)2
2206.8	(Hex)2 (HexNAc)2 (NeuAc)1 + (Man)3(GlcNAc)2
2220.8	(HexNAc)3 (Deoxyhexose)3 + (Man)3(GlcNAc)2
2352.9	(Hex)2 (HexNAc)2 (Deoxyhexose)1 (NeuAc)1 + (Man)3(GlcNAc)2
2489.9	(Hex)5 (HexNAc)1 (NeuAc)1 + (Man)3(GlcNAc)2
2493.9	(Hex)1 (HexNAc)5 (Deoxyhexose)1 + (Man)3(GlcNAc)2
2497.9	(Hex)2 (HexNAc)2 (Deoxyhexose)2 (NeuAc)1 + (Man)3(GlcNAc)2
2511.9	(Hex)2 (HexNAc)2 (NeuAc)2 + (Man)3(GlcNAc)2
2519.9	(Hex)4 (HexNAc)2 (Deoxyhexose)2 + (Man)3(GlcNAc)2
2527.9	(Hex)1 (HexNAc)3 (Deoxyhexose)4 + (Man)3(GlcNAc)2
2533.9	(Hex)5 (HexNAc)2 (Deoxyhexose)1 + (Man)3(GlcNAc)2 (Hex)3 (Deoxyhexose)6 + (Man)3(GlcNAc)2
2556.0	(Hex)2 (HexNAc)3 (Deoxyhexose)1 (NeuAc)1 + (Man)3(GlcNAc)2
2572.0	(Hex)3 (HexNAc)3 (NeuAc)1 + (Man)3(GlcNAc)2
2658.0	(Hex)2 (HexNAc)2 (Deoxyhexose)1 (NeuAc)2 + (Man)3(GlcNAc)2
2748.0	(Hex)2 (HexNAc)4 (Deoxyhexose)3 + (Man)3(GlcNAc)2 (Hex)2 (HexNAc)1 (Deoxyhexose)3 (NeuAc)2 + (Man)3(GlcNAc)2
2861.1	(Hex)2 (HexNAc)6 (Deoxyhexose)1 + (Man)3(GlcNAc)2 (Hex)2 (HexNAc)3 (Deoxyhexose)1 (NeuAc)2 + (Man)3(GlcNAc)2
2877.1	(Hex)3 (HexNAc)3 (NeuAc)2 + (Man)3(GlcNAc)2 (Hex)1 (HexNAc)1 (Deoxyhexose)5 (NeuAc)2 + (Man)3(GlcNAc)2
3182.2	(Hex)3 (HexNAc)3 (NeuAc)3 + (Man)3(GlcNAc)2

[a] ND: not determined.

were observed (Figure 2B,C). However, progression-free survival (PFS) was significantly longer in the high FUCA activity group (>4.3 U/L) than in the low FUCA activity group ($p < 0.05$, Figure 2D). Although plasma FUCA activity was not correlated with the clinical response to trastuzumab, it may be useful as a biomarker for predicting the PFS of for trastuzumab treatment.

Low Expression of Plasma 2534 m/z N-Glycan Correlated with Unfavorable Clinical Outcome. We collected plasma N-glycans using glycoblotting-based glycan enrichment[31] and measured their MALDI-TOF-MS peaks. Thirty-one major peaks of N-glycan, observed in over 50% of the patients, were identified (Table 2). Representative data are shown in Figure 3 (left panel). A statistical analysis comparing each peak with the clinical outcome revealed that the expression of plasma 2534 m/z N-glycan was significantly lower in patients with progressive disease (PD) ($p < 0.05$, Figure 4A). Low expression of 2534 m/z N-glycan discriminated between PD and non-PD with 75% sensitivity and 82% specificity. The expressions of plasma 2534 m/z N-glycan in the PD and non-PD groups were 4.3 ± 8.1 and 16.1 ± 11.6 (% of control), respectively. Representative data of 2534 m/z N-glycan from six patients are shown in Figure 3 (right panel). In addition, patients with a low expression (not detectable at 2534 m/z) of plasma 2534 m/z N-glycan exhibited a significantly short PFS ($p < 0.05$, Figure 4B). These results suggest that a low plasma 2534 m/z N-glycan level is associated with a poor clinical outcome and that plasma 2534 m/z N-glycan may be a predictive biomarker in breast cancer patients treated with trastuzumab.

Discussion

In this study, we investigated predictive biomarkers of response to trastuzumab monotherapy in breast cancer patients, focusing on the processes of fucosylation and glycosylation. Shah et al. reported that serum FUCA activity levels varied in normal, precancerous, and malignant conditions, and suggested that serum FUCA activity might be a useful marker for early detection and for monitoring treatment response in oral cancer patients.[32] We found that a higher plasma FUCA activity level was correlated with a favorable PFS, but that the plasma FUT8 levels was not correlated with clinical response and PFS in breast cancer patients who received trastuzumab treatment. Although the precise mechanisms responsible for our results remain unclear, we speculated that the resulting plasma FUT8 level was not correlated with the clinical outcome because FUT8 catalytic activity occurs strictly in the Golgi apparatus and requires GDP-fucose. On the other hand, the FUCA enzyme has two isoforms, FUCA1 (fucosidase, alpha-L-1, tissue) and FUCA2 (fucosidase, alpha-L-2, plasma). Because FUCA2 is secreted into the plasma,[33] it may influence the phenotype of cancer cells, thereby explaining its correlation with clinical outcome. Indeed, the mRNA expression of FUCA2 was higher and that of FUCA1 was lower in biopsy specimens of gastric cancer, compared with paired noncancerous gastric mucosa (data not shown).

Many researchers have reported new methods for performing glycan structural analyses using mass spectrometry.[34,35] Our method of examining N-glycan profiles utilizes only small amount of plasma sample, making it easy to analyze clinical samples. Several reports have demonstrated that analyzing the glycan structures of proteins in human sera can reveal novel tumor markers in cancer.[11,36] Kyselova et al. reported that several N-glycan structures appear to indicate cancer progression in breast cancer, suggesting that N-glycan profiling of serum may be a useful approach for staging the progression of cancer.[37] An et al. reported that oligosaccharide profiling data using sera samples from patients with ovarian cancer patients and normal controls demonstrated the presence of several unique serum glycan markers in all the patients but not in the normal samples.[38] They mentioned that one major advantage of this approach is that the glycans can be examined

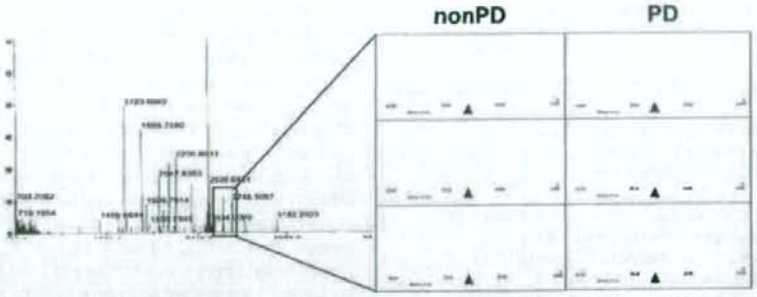

Figure 3. Representative data of plasma N-glycan profile measured using MALDI-TOF-MS (left panel). Twenty-seven microliters of plasma sample was used for the analysis. The mixture was trypsinized and reacted using *N*-glycosidase F. Internal N-glycan standard was added, and the mixture was purified using glycoblotting-based glycan enrichment. The purified samples were measured using MALDI-TOF-MS in reflector, positive ion mode. The number of laser shots was 300 × 2 shots, and the mass range acquired was 700–5000 Da. The N-glycan structure was determined using the GlycoSuite online database, proteome System. All the plasma N-glycans peaks obtained from MALDI-TOF-MS were normalized using the internal standard. The identified 2534 *m/z* N-glycan peaks are shown in six plasma samples (right panel). ▲, 2534 *m/z*; PD, progressive disease.

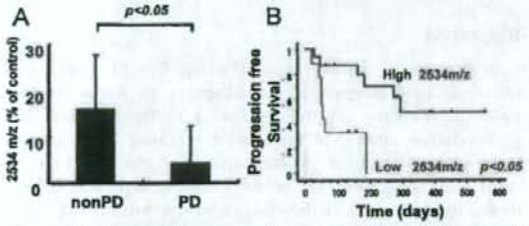

Figure 4. Plasma 2534 *m/z* N-glycan and clinical outcome. (A) Expression of plasma 2534 *m/z* N-glycan and clinical response. The expression of plasma 2534 *m/z* N-glycan was significantly lower ($p < 0.05$) in patients with progressive disease (PD). (B) Kaplan–Meier curve of high (detectable) or low (not detectable) plasma 2534 *m/z* N-glycan groups for progression-free survival (PFS) after trastuzumab treatment. The patients with a low expression of plasma 2534 *m/z* N-glycan exhibited a significantly shorter PFS ($p < 0.05$).

using a serum samples, and cancer biopsy specimens are not needed. In the present study, when the plasma N-glycan profiles of breast cancer patients were examined using MALDI-TOF-MS, 2534 *m/z* N-glycan was found to be correlated with clinical response and PFS. The estimated structure of the identified 2534 *m/z* N-glycan is (Hex)5(HexNAc)2(Deoxyhexose)1 + (Man)3(GlcNAc)2 according to a database (http://au.expasy.org/tools/glycomod/). The experimental confirmation of the predicted structure of 2534 *m/z* is very important. Although we no longer have enough plasma samples to determine the experimental confirmation of structure, we plan to examine 2534 N-glycan in clinical samples to give the experimental confirmation in the future prospective study. This N-glycan has also been found in plasma samples from patients with pancreas cancer, pancreatitis and obstructive bile duct disease (data not shown). We are now investigating the biological mechanism of this N-glycan modification.

In conclusion, we demonstrated that plasma FUCA activity and plasma N-glycan are correlated with the clinical outcome of breast cancer patients treated with trastuzumab. N-Glycan profiles raise the possibility of identifying novel predictive biomarkers for antibody therapy, although a validation study with a larger sample size is needed. Our results show the utility of glycosylation analysis for clinical cancer therapy and provide a novel insight into biomarker studies using glycobiological tools in the field of breast cancer.

Acknowledgment. The following people have played very important roles in the outcome of this project: Hisao Fukumoto, Tatsu Shimoyama, Naoki Hayama, Hideharu Kimura, Masayuki Takeda, Junya Fukai, Kazuko Sakai and Terufumi Kato. We also thank Dr. Richard Simon and Dr. Amy Peng for providing the BRB ArrayTools software. We thank Mr. Hideyuki Shimaoka and Mr. Kazuhiko Fujiwara (Sumitomo Bakelite Co., Ltd.) for their technical support and useful advice. We also thank Mrs. Eiko Honda (Life Science Research Institute, Kinki University) for assistance with the experiments. This work was supported by funds for Health and Labor Scientific Research Grants, Research on Advanced Medical Technology H17-Pharmaco-006 and for the Third-Term Comprehensive 10-Year Strategy for Cancer Control. K.M. is the recipient of a Research Resident Fellowship from the Foundation of Promotion of Cancer Research in Japan.

References

(1) Hakomori, S. Glycosylation defining cancer malignancy: new wine in an old bottle. *Proc. Natl. Acad. Sci. U.S.A.* **2002**, *99* (16), 10231–3.

(2) Ono, M.; Hakomori, S. Glycosylation defining cancer cell motility and invasiveness. *Glycoconjugate J.* **2004**, *20* (1), 71–8.

(3) Zhao, Y. Y.; Takahashi, M.; Gu, J. G.; Miyoshi, E.; Matsumoto, A.; Kitazume, S.; Taniguchi, N. Functional roles of N-glycans in cell signaling and cell adhesion in cancer. *Cancer Sci.* **2008**, *99* (7), 1304–10.

(4) Hakomori, S. Tumor malignancy defined by aberrant glycosylation and sphingo(glyco)lipid metabolism. *Cancer Res.* **1996**, *56* (23), 5309–18.

(5) Contessa, J. N.; Bhojani, M. S.; Freeze, H. H.; Rehemtulla, A.; Lawrence, T. S. Inhibition of N-linked glycosylation disrupts receptor tyrosine kinase signaling in tumor cells. *Cancer Res.* **2008**, *68* (10), 3803–9.

(6) Guo, H. B.; Randolph, M.; Pierce, M. Inhibition of a specific N-glycosylation activity results in attenuation of breast carcinoma cell invasiveness-related phenotypes: inhibition of epidermal growth factor-induced dephosphorylation of focal adhesion kinase. *J. Biol. Chem.* **2007**, *282* (30), 22150–62.

(7) Qiu, Y.; Patwa, T. H.; Xu, L.; Shedden, K.; Misek, D. E.; Tuck, M.; Jin, G.; Ruffin, M. T.; Turgeon, D. K.; Synal, S.; Bresalier, R.; Marcon, N.; Brenner, D. E.; Lubman, D. M. Plasma glycoprotein profiling for colorectal cancer biomarker identification by lectin glycoarray and lectin blot. *J. Proteome Res.* **2008**, *7* (4), 1693–703.

(8) Abbott, K. L.; Aoki, K.; Lim, J. M.; Porterfield, M.; Johnson, R.; O'Regan, R. M.; Wells, L.; Tiemeyer, M.; Pierce, M. Targeted glycoproteomic identification of biomarkers for human breast carcinoma. *J. Proteome Res.* **2008**, *7* (4), 1470–80.
(9) Heo, S. H.; Lee, S. J.; Ryoo, H. M.; Park, J. Y.; Cho, J. Y. Identification of putative serum glycoprotein biomarkers for human lung adenocarcinoma by multilectin affinity chromatography and LC-MS/MS. *Proteomics* **2007**, *7* (23), 4292–302.
(10) Nakagawa, T.; Uozumi, N.; Nakano, M.; Mizuno-Horikawa, Y.; Okuyama, N.; Taguchi, T.; Gu, J.; Kondo, A.; Taniguchi, N.; Miyoshi, E. Fucosylation of N-glycans regulates the secretion of hepatic glycoproteins into bile ducts. *J. Biol. Chem.* **2006**, *281* (40), 29797–806.
(11) Ueda, K.; Katagiri, T.; Shimada, T.; Irie, S.; Sato, T. A.; Nakamura, Y.; Daigo, Y. Comparative profiling of serum glycoproteome by sequential purification of glycoproteins and 2-nitrobenzenesulfenyl (NBS) stable isotope labeling: a new approach for the novel biomarker discovery for cancer. *J. Proteome Res.* **2007**, *6* (9), 3475–83.
(12) Li, D.; Mallory, T.; Satomura, S. AFP-L3: a new generation of tumor marker for hepatocellular carcinoma. *Clin. Chim. Acta* **2001**, *313* (1–2), 15–9.
(13) Yamaguchi, Y.; Fujii, J.; Inoue, S.; Uozumi, N.; Yanagidani, S.; Ikeda, Y.; Egashira, M.; Miyoshi, O.; Niikawa, N.; Taniguchi, N. Mapping of the alpha-1,6-fucosyltransferase gene, FUT8, to human chromosome 14q24.3. *Cytogenet. Cell Genet.* **1999**, *84* (1–2), 58–60.
(14) Yamane-Ohnuki, N.; Kinoshita, S.; Inoue-Urakubo, M.; Kusunoki, M.; Iida, S.; Nakano, R.; Wakitani, M.; Niwa, R.; Sakurada, M.; Uchida, K.; Shitara, K.; Satoh, M. Establishment of FUT8 knockout Chinese hamster ovary cells: an ideal host cell line for producing completely defucosylated antibodies with enhanced antibody-dependent cellular cytotoxicity. *Biotechnol. Bioeng.* **2004**, *87* (5), 614–22.
(15) Niwa, R.; Hatanaka, S.; Shoji-Hosaka, E.; Sakurada, M.; Kobayashi, Y.; Uehara, A.; Yokoi, H.; Nakamura, K.; Shitara, K. Enhancement of the antibody-dependent cellular cytotoxicity of low-fucose IgG1 is independent of FcgammaRIIIa functional polymorphism. *Clin. Cancer Res.* **2004**, *10* (18 Pt 1), 6248–55.
(16) Suzuki, E.; Niwa, R.; Saji, S.; Muta, M.; Hirose, M.; Iida, S.; Shiotsu, Y.; Satoh, M.; Shitara, K.; Kondo, M.; Toi, M. A nonfucosylated anti-HER2 antibody augments antibody-dependent cellular cytotoxicity in breast cancer patients. *Clin. Cancer Res.* **2007**, *13* (6), 1875–82.
(17) Giardina, M. G.; Matarazzo, M.; Morante, R.; Lucariello, A.; Varriale, A.; Guardasole, V.; De Marco, G. Serum alpha-L-fucosidase activity and early detection of hepatocellular carcinoma: a prospective study of patients with cirrhosis. *Cancer.* **1998**, *83* (12), 2468–74.
(18) Ayude, D.; Paez De La Cadena, M.; Martinez-Zorzano, V. S.; Fernandez-Briera, A.; Rodriguez-Berrocal, F. J. Preoperative serum alpha-L-fucosidase activity as a prognostic marker in colorectal cancer. *Oncology* **2003**, *64* (1), 36–45.
(19) Ayude, D.; Fernandez-Rodriguez, J.; Rodriguez-Berrocal, F. J.; Martinez-Zorzano, V. S.; de Carlos, A.; Gil, E.; Paez de La Cadena, M. Value of the serum alpha-L-fucosidase activity in the diagnosis of colorectal cancer. *Oncology* **2000**, *59* (4), 310–6.
(20) Slamon, D. J.; Clark, G. M.; Wong, S. G.; Levin, W. J.; Ullrich, A.; McGuire, W. L. Human breast cancer: correlation of relapse and survival with amplification of the HER-2/neu oncogene. *Science* **1987**, *235* (4785), 177–82.
(21) Seshadri, R.; Firgaira, F. A.; Horsfall, D. J.; McCaul, K.; Setlur, V.; Kitchen, P. Clinical significance of HER-2/neu oncogene amplification in primary breast cancer. The South Australian Breast Cancer Study Group. *J Clin Oncol.* **1993**, *11* (10), 1936–42.
(22) Menard, S.; Pupa, S. M.; Campiglio, M.; Tagliabue, E. Biologic and therapeutic role of HER2 in cancer. *Oncogene* **2003**, *22* (42), 6570–8.
(23) Vogel, C. L.; Cobleigh, M. A.; Tripathy, D.; Gutheil, J. C.; Harris, L. N.; Fehrenbacher, L.; Slamon, D. J.; Murphy, M.; Novotny, W. F.; Burchmore, M.; Shak, S.; Stewart, S. J.; Press, M. Efficacy and safety of trastuzumab as a single agent in first-line treatment of HER2-overexpressing metastatic breast cancer. *J. Clin. Oncol.* **2002**, *20* (3), 719–26.
(24) Hurley, J.; Doliny, P.; Reis, I.; Silva, O.; Gomez-Fernandez, C.; Velez, P.; Pauletti, G.; Powell, J. E.; Pegram, M. D.; Slamon, D. J. Docetaxel, cisplatin, and trastuzumab as primary systemic therapy for human epidermal growth factor receptor 2-positive locally advanced breast cancer. *J. Clin. Oncol.* **2006**, *24* (12), 1831–8.
(25) Naruse, I.; Fukumoto, H.; Saijo, N.; Nishio, K. Enhanced anti-tumor effect of trastuzumab in combination with cisplatin. *Jpn. J. Cancer Res.* **2002**, *93* (5), 574–81.
(26) Kimura, H.; Sakai, K.; Arao, T.; Shimoyama, T.; Tamura, T.; Nishio, K. Antibody-dependent cellular cytotoxicity of cetuximab against tumor cells with wild-type or mutant epidermal growth factor receptor. *Cancer Sci.* **2007**, *98* (8), 1275–80.
(27) Kimura, H.; Kasahara, K.; Kawaishi, M.; Kunitoh, H.; Tamura, T.; Holloway, B.; Nishio, K. Detection of epidermal growth factor receptor mutations in serum as a predictor of the response to gefitinib in patients with non-small-cell lung cancer. *Clin. Cancer Res.* **2006**, *12* (13), 3915–21.
(28) Arao, T.; Fukumoto, H.; Takeda, M.; Tamura, T.; Saijo, N.; Nishio, K. Small in-frame deletion in the epidermal growth factor receptor as a target for ZD6474. *Cancer Res.* **2004**, *64* (24), 9101–4.
(29) Matsumoto, K.; Yokote, H.; Arao, T.; Maegawa, M.; Tanaka, K.; Fujita, Y.; Shimizu, C.; Hanafusa, T.; Fujiwara, Y.; Nishio, K. N-Glycan fucosylation of epidermal growth factor receptor modulates receptor activity and sensitivity to epidermal growth factor receptor tyrosine kinase inhibitor. *Cancer Sci.* **2008**, *99* (8), 1611–17.
(30) Uozumi, N.; Teshima, T.; Yamamoto, T.; Nishikawa, A.; Gao, Y. E.; Miyoshi, E.; Gao, C. X.; Noda, K.; Islam, K. N.; Ihara, Y.; Fujii, S.; Shiba, T.; Taniguchi, N. A fluorescent assay method for GDP-L-Fuc:N-acetyl-beta-D-glucosaminide alpha 1→6fucosyltransferase activity, involving high performance liquid chromatography. *J. Biochem.* **1996**, *120* (2), 385–92.
(31) Miura, Y.; Hato, M.; Shinohara, Y.; Kuramoto, H.; Furukawa, J.; Kurogochi, M.; Shimaoka, H.; Tada, M.; Nakanishi, K.; Ozaki, M.; Todo, S.; Nishimura, S. BlotGlycoABCTM, an integrated glycoblotting technique for rapid and large scale clinical glycomics. *Mol. Cell. Proteomics* **2008**, *7* (2), 370–7.
(32) Shah, M.; Telang, S.; Raval, G.; Shah, P.; Patel, P. S. Serum fucosylation changes in oral cancer and oral precancerous conditions: alpha-L-fucosidase as a marker. *Cancer* **2009**, *115* (2), 336–46.
(33) Ng, W. G.; Donnell, G. N.; Koch, R.; Bergren, W. R. Biochemical and genetic studies of plasma and leukocyte alpha-L-fucosidase. *Am. J. Hum. Genet.* **1976**, *28* (01), 42–50.
(34) Zhao, J.; Qiu, W.; Simeone, D. M.; Lubman, D. M. N-linked glycosylation profiling of pancreatic cancer serum using capillary liquid phase separation coupled with mass spectrometric analysis. *J. Proteome Res.* **2007**, *6* (3), 1126–38.
(35) Zhao, J.; Simeone, D. M.; Heidt, D.; Anderson, M. A.; Lubman, D. M. Comparative serum glycoproteomics using lectin selected sialic acid glycoproteins with mass spectrometric analysis: application to pancreatic cancer serum. *J. Proteome Res.* **2006**, *5* (7), 1792–802.
(36) Isailovic, D.; Kurulugama, R. T.; Plasencia, M. D.; Stokes, S. T.; Kyselova, Z.; Goldman, R.; Mechref, Y.; Novotny, M. V.; Clemmer, D. E. Profiling of human serum glycans associated with liver cancer and cirrhosis by IMS-MS. *J. Proteome Res.* **2008**, *7* (3), 1109–17.
(37) Kyselova, Z.; Mechref, Y.; Kang, P.; Goetz, J. A.; Dobrolecki, L. E.; Sledge, G. W.; Schnaper, L.; Hickey, R. J.; Malkas, L. H.; Novotny, M. V. Breast cancer diagnosis and prognosis through quantitative measurements of serum glycan profiles. *Clin Chem.* **2008**, *54* (7), 1166–75.
(38) An, H. J.; Miyamoto, S.; Lancaster, K. S.; Kirmiz, C.; Li, B.; Lam, K. S.; Leiserowitz, G. S.; Lebrilla, C. B. Profiling of glycans in serum for the discovery of potential biomarkers for ovarian cancer. *J. Proteome Res.* **2006**, *5* (7), 1626–35.

PR800655P

Identification of prognostic biomarkers in gastric cancer using endoscopic biopsy samples

Yasuhide Yamada,[1] Tokuzo Arao,[2] Takuji Gotoda,[3] Hirokazu Taniguchi,[4] Ichiro Oda,[3] Kuniaki Shirao,[1] Yasuhiro Shimada,[1] Tetsuya Hamaguchi,[1] Ken Kato,[1] Tetsutaro Hamano,[7] Fumiaki Koizumi,[5] Tomohide Tamura,[1] Daizo Saito,[3] Tadakazu Shimoda,[4] Makoto Saka,[6] Takeo Fukagawa,[6] Hitoshi Katai,[6] Takeshi Sano,[6] Mitsuru Sasako[6] and Kazuto Nishio[2,8]

[1]Medical Oncology, [2]Endoscopic Division, [4]Diagnostic Pathology Division, [5]Shien Lab, and [6]Surgical Division, National Cancer Center Hospital, 5-1-1 Tsukiji, Chuo-ku, Tokyo 104-0045; [3]Department of Genome Biology, Kinki University School of Medicine, 377-2 Ohno-Higashi, Osaka-Sayama, Osaka 589-8511; [7]Hamano Statistical Analysis Ltd, 6-7-15 Chuo-cho, Higashikurume, Tokyo 203-0054, Japan

(Received June 22, 2008/Revised July 16, 2008/Accepted July 16, 2008/Online publication September 28, 2008)

Endoscopic biopsy prior to chemotherapy provides an opportunity for studying biomarkers to predict the overall survival in gastric cancer patients. This prospective study was performed to identify prognostic biomarkers in patients with unresected gastric cancer. Fifty-nine cases of chemotherapy-naive metastatic gastric cancer were enrolled in this study. A microarray analysis was performed using 40 biopsy samples to identify candidate genes whose expressions might be correlated with the overall survival. After adjusting for clinical covariates based on a multivariate analysis, the identified genes were validated using real-time reverse transcription polymerase chain reaction (RT-PCR) analysis in 19 independent validation samples. Ninety-eight candidate genes whose expression levels were significantly correlated with the overall survival were identified using a microarray analysis based on a proportional hazards model ($P < 0.005$). Multivariate analysis was performed to assess 10 of these genes, and the results yielded a statistical significance level for *DACH1* and *PDCD6*. We further evaluated these two genes in independent samples using real-time RT-PCR and found that lower mRNA expression levels of *PDCD6* were correlated significantly with a poor overall survival. We identified *PDCD6* as a prognostic biomarker in patients with unresected gastric cancer using endoscopic biopsy samples. Our PCR-based single gene prediction strategy successfully predicted the overall survival and may lead to a better understanding of this disease subgroup. (*Cancer Sci* 2008; 99: 2193–2199)

Over the past two decades, various anticancer agents have been examined for their efficacy against gastric cancer, including 5-fluorouracil (5-FU) and 5-FU-based drugs, taxanes, CPT-11 and cisplatin, all administered either as monotherapy or in combination regimens;[1] however, the median survival time (MST) of these patients remains at only approximately 7 months.[2,3] In a recent randomized phase III trial examining oral S-1 monotherapy and cisplatin plus irinotecan combination therapy, the response rates to both S-1 and to the cisplatin plus irinotecan combination therapy were approximately 50%, indicating that around half of the patients did not respond to chemotherapy,[4–7] and the MST in both the arms was less than 1 year.[8] Thus, the prognosis of patients with gastric cancer remains poor.

The commonly recognized prognostic factors in cases of unresectable gastric cancer are the performance status, presence/absence of liver metastases, presence/absence of peritoneal metastases and the serum levels of alkaline phosphatase.[9] Many molecular biomarkers have been also investigated for their potential to predict the outcome in hypothesis-based studies. Several studies have shown that the mRNA levels and immunohistochemical staining intensity of thymidylate synthase (TS) in gastric cancers treated with fluorouracil are associated with the response and survival; in addition, the excision repair cross-complementing (ERCC)1 gene expression level has been shown to be associated with the clinical outcome in patients treated with cisplatin.[10,11] HER2 expression has also been reported to be a prognostic marker in cases of differentiated gastric cancer.[12,13] Mutation of p53 and high p53 protein expression, and high expression levels of urokinase-plasminogen activator, xanthine oxidoreductase, claudin-4, vascular endothelial growth factor, interleukin-8 and cyclin E have all been correlated with poor survival.[13–19] In terms of epigenetic alterations, reduced expression of acetylated histone H4 or DNA methylation of CDH1 and RAR-β have been shown to be correlated with tumor invasiveness and the tumor metastasizing potential.[20,21]

On the other hand, the recent introduction of the microarray technology has enabled significant genes to be identified almost throughout the genome using a hypothesis-free approach. The possibility of performing genome-wide searches is a major advantage, and such searches may be the only way to discover genes that would otherwise be unlikely to even be suggested as candidates. In gastric cancer, biopsy samples of the primary lesions can be easily obtained by endoscopy prior to treatment; however, few prospective biomarker studies using endoscopic biopsy samples to predict patient outcome have been performed to date. Therefore, we conducted a prospective study to identify biomarkers for predicting survival in patients with unresected metastatic gastric cancer.

Materials and Methods

Patients and samples. The eligible subjects in this study were patients with histologically confirmed, untreated and metastatic stage IV gastric cancer between 20 and 75 years of age. Additional inclusion criteria included an Eastern Cooperative Oncology Group performance status of 0–2. The exclusion criteria included history of prior chemotherapy or major surgery. All patients received chemotherapy using a 5-FU-based regimen (5-FU alone, S1 alone, 5-FU + methotrexate, 5-FU + cisplatin, or S1 + cisplatin) or a CPT-11 plus cisplatin regimen. Sixty-five gastric cancer patients were enrolled in the study. Of these, two were excluded because of insufficient RNA quantities extracted from their biopsy specimens, and four were excluded because of the poor RNA quality. Thus, samples from the remaining 59 patients were analyzed. The survival time was followed after the patients were initiated on chemotherapy. This study was approved

[8]To whom correspondence should be addressed. E-mail: knishio@med.kindai.ac.jp

doi: 10.1111/j.1349-7006.2008.00935.x

by the Institutional Review Board of the National Cancer Center Hospital, and written informed consent was obtained from all the patients.

The endoscopic biopsy samples collected were immediately placed in an RNA stabilization solution (Isogen; Nippongene, Tokyo, Japan) and stored at −80°C. Other biopsy samples obtained from the same location were reviewed by a pathologist to confirm the presence of tumor cells. The RNA extraction method and the quality check protocol have been described previously.[22]

Study design. This prospective study was started in July 2003 and enrollment was completed in November 2006 at the National Cancer Center Hospital. Fifty-nine gastric cancer samples were evaluated in this study. The samples were divided into a training set ($n = 40$) and a validation set ($n = 19$; 2:1) using computer-generated randomization (Microsoft Office Excel, Microsoft, Redmond, WA, USA). A microarray analysis was performed using the training set of 40 samples, and candidate genes whose expressions were correlated with the overall survival were identified. Multivariate analysis was performed to adjust the expression of 10 of these candidate genes for clinical features. Finally, the significant genes were evaluated in an independent set of 19 samples and survival was predicted using the results of real-time reverse transcription polymerase chain reaction (RT-PCR) analyses.

Real-time RT-PCR. Real-time RT-PCR was performed for 10 genes: *DACH1* (dachshund homolog 1, NM_004392); *EGFR* (epidermal growth factor receptor, NM_005228); *MT1X* (metallothionein 1X, NM_005952); *YWHAE* (tyrosine 3-monooxygenase/tryptophan 5-monooxygenase activation protein, epsilon polypeptide, NM_006761); *GPX3* (glutathione peroxidase 3, NM_002084); *PDCD6* (programmed cell death 6, NM_013232); *WDR33* (WD repeat domain 33, NM_018383); *C14orf43* (chromosome 14 open reading frame 43, NM_194278); *MYLIP* (myosin regulatory light chain interacting protein, NM_013262); and *GKAP1* (G kinase anchoring protein 1, NM_025211). Glyceraldehyde 3 phosphate dehydrogenase (*GAPD*, NM_002046) was used to normalize the expression levels in the subsequent quantitative analyses. RNA was converted to cDNA using a GeneAmp RNA PCR Core kit (Applied Biosystems, Foster City, CA). The transcripts were quantified using the Power SYBR Green PCR Master Mix (Applied Biosystems) and 7900HT Fast Real-time PCR system (Applied Biosystems) and reported relative to the *GAPD* expression levels. The PCR conditions were as follows: one cycle of denaturation at 95°C for 10 min, followed by 40 cycles at 95°C for 15 s and 60°C for 60 s. To amplify the target genes, the following primers were purchased from Takara (Yotsukaichi, Japan): DACH1-FW, 5′-AAG GGC TGC TAA AGC AAT CAG G-3′, and DACH1-RW, 5′-CTT TGT GGC AAA GCG ACA TTA GG-3′; EGFR-FW, 5′-GGT GCG AAT GAC AGT AGC ATT ATG A-3′, and EGFR-RW, 5′-AAA TGG GCT CCT AAC TAG CTG AAT C-3′; MT1X-FW, 5′-TTG ATC GGG AAC TCC TGC TTC T-3′, and MT1X-RW, 5′-ACA CTT GGC ACA GCC GAC A-3′; GPX3-FW, 5′-ATG CCT ACA GGT ATG CGT GAT TG-3′, and GPX3-RW, 5′-TGC AGG CAC ACA GAT GGT ACA-3′; PDCD6-FW, 5′-TCA AGG CCA GAC TAG ATC AGC CTA A-3′, and PDCD6-RW, 5′-GCT GGG ATG AGG CAC ATG AC-3′; YWHAE-FW, 5′-GGC AGA ATT TGC CAC AGG AA-3′, and YWHAE-RW, 5′-ACC TAA GCG AAT AGG ATG CGT TG-3′; WDR33-FW, 5′-ATG CAT GGG CTC TGT CAG TTT C-3′, and WDR33-RW, 5′-GGC TGA TAC CGG GAC AAC ACT AC-3′; C14orf43-FW, 5′-CAG ACT GGC AAG CCT AAC TCC ATA-3′, and C14orf43-RW, 5′-CAA GGC TGT TCC TGT GCT CTG-3′; MYLIP-FW, 5′-ACG TCT ATC TGC CAA CGC ACA C-3′, and MYLIP-RW, 5′-CAG TTC ATG GAA ACA TGC CAA GTC-3′; GKAP1-FW, 5′-TTG CGA ATA AGT TTC GGA GCA TC-3′, and GKAP1-RW, 5′-GCC ACT GCC ACT ATC CAC TTG TAA-3′; GAPD-FW, 5′-GCA CCG TCA AGG CTG AGA AC-3′, and GAPD-RW, 5′-ATG GTG GTG AAG ACG CCA GT-3′.

Oligonucleotide microarray study. The microarray procedure was performed according to the Affymetrix protocols (Santa Clara, CA). In brief, the total RNA extracted from the tumor samples was analyzed using an Agilent 2100 Bioanalyzer (Agilent Technologies, Waldbronn, Germany) for quality check, and cRNA was synthesized using the GeneChip 3′-Amplification Reagents One-Cycle cDNA Synthesis Kit (Affymetrix). The labeled cRNA were then purified and used for construction of the probes. Hybridization was performed using the Affymetrix GeneChip HG-U133 Plus 2.0 array for 16 h at 45°C. The signal intensities were measured using a GeneChip Scanner3000 (Affymetrix) and converted to numerical data using the GeneChip Operating Software, ver. 1 (Affymetrix).

Statistical analysis. The microarray analysis was performed using the BRB Array Tools software ver. 3.3.0 (http://linus.nci.nih.gov/BRB-ArrayTools.html) developed by Dr Richard Simon and Dr Amy Peng. In brief, a log base 2 transformation was applied to the raw microarray data, and global normalization was used to calculate the median over the entire array. Genes were excluded if the percentage of data missing or filtered out exceeded 20%. Genes that passed the filtering criteria were then considered for further analysis. We computed a statistical significance level ($P < 0.005$) for each gene based on a univariate proportional hazards model.

To adjust the expression of 10 genes (*DACH1*, *EGFR*, *MT1X*, *YWHAE*, *GPX3*, *PDCD6*, *WDR33*, *C14orf43*, *MYLIP* and *GKAP1*) for clinical features (age, sex, performance status [PS], number of metastatic sites, received chemotherapy), clinical data and the normalized microarray expression data of the 10 genes were imported into SAS software ver. 9.1.3 (SAS Institute, Cary, NC, USA) and a Cox regression model was constructed for multivariate analysis against each of the variables. The study groups were divided into two groups based on each of the clinical features: age (<65 or ≥65 years), sex (male or female), PS (0 or ≥1), number of metastatic sites (<3 or ≥3), chemotherapy (5-FU-based or CPT11 + CDDP) and expression levels of 10 genes). $P < 0.05$ was considered significant.

Results

Identification of 98 candidate prognosis-related genes using a microarray analysis. The univariate analysis of clinical features including age (<65 or ≥65 years), sex, PS (0 or ≥1), number of metastatic sites (1, 2 or ≥3) and received chemotherapy (5-FU-based or CPT11 + CDDP) were performed for 40 microarray samples (Table 1). There were no significant differences between any of the two groups divided according to age, sex, number of metastatic sites or received chemotherapy; however, significant differences were noted between the two groups divided according to PS ($P = 0.048$).

To identify the candidate prognosis-related genes from amongst over 47 000 transcripts, a microarray analysis was performed for a training set of 40 samples. A total of 21 308 genes passed the filtering criteria and were further analyzed. Ninety-eight genes were significantly correlated with survival, according to a Cox proportional hazards model ($P < 0.005$) (Table 2). Fifty-nine genes were protective genes (hazard ratio, <1), and 39 were risk genes (hazard ratio >1).

A heat-map of the expression values of the 98 selected genes comparing the unfavorable prognosis group (survival time, <180 days) and favorable prognosis group (survival time, ≥180 days) is shown in Fig. 1. Genes are plotted via hierarchical clustering.

Multivariate analysis of prognosis-related genes. Of the 98 candidate genes, we prioritized those that: (i) were selected by overlapping probes; (ii) were novel genes; or (iii) had a lower

doi: 10.1111/j.1349-7006.2008.00935.x

Table 1. Univariate analysis of clinical features

Variable	No. of patients	MST (days)	*P*-value (log-rank test)
Age (years)			
≥65	16	235	0.454
<65	24	250	
Sex			
Male	29	243	0.926
Female	11	267	
PS			
≥1	24	182	0.048
0	16	309	
Metastasis			
1, 2	10	137	0.102
≥3	30	261	
Chemotherapy			
5-FU-based	26	245	0.594
CPT11 + CDDP	14	240	

MST, median survival time; PS, performance status.

P-value according to a Cox proportional hazards model. We selected the following 10 genes of interest for real-time RT-PCR analysis: *DACH1*, *EGFR*, *MT1X*, *YWHAE*, *GPX3*, *PDCD6*, *WDR33*, *C14orf43*, *MYLIP* and *GKAP1*.

To adjust for relevant clinical covariates against these 10 genes, we performed a multivariate analysis (Table 3). The results of the multivariate analysis revealed that high *DACH1* expression and high *PDCD6* expression were significantly correlated with the favorable outcome ($P = 0.0134$ and $P = 0.0015$, respectively). We therefore considered that the *DACH1* and *PDCD6* expressions were independent prognostic markers from the results of the multivariate analysis. Results of microarray data and patient survival in the training set of 40 patients are shown in Fig. 2. The Kaplan–Meier method was used for *DACH1* and *PDCD6*. The low *PDCD6* and *DACH1* expression groups had significantly poorer outcomes ($P < 0.0001$ and $P = 0.0045$).

Validation using real-time RT-PCR in independent samples. The mRNA expression levels of *DACH1* and *PDCD6* were quantified using real-time RT-PCR in 19 independent samples to validate the results of the microarray. While the expression levels of *DACH1* were not correlated with survival, those of *PDCD6* in independent samples were significantly correlated with the survival ($P = 0.007$) (Table 4). The Kaplan–Meier method was used to estimate the overall survival using the median value (Fig. 3a). All quantified expression levels of real time RT-PCR data are shown as Fig. 3(b). The mRNA expressions of *PDCD6* varied by approximately 25 fold (range, 0.98–25.1). The low *PDCD6* expression groups had significantly poorer outcomes ($P = 0.0018$). We concluded that *PDCD6* was a valuable gene for predicting the survival in patients with gastric cancer. These results indicate that our PCR-based single gene prediction strategy using endoscopic biopsy samples could successfully predict the overall patient survival.

Discussion

Several studies have identified prognostic biomarkers in cases of gastric cancer using microarray analysis. Hasegawa *et al.* identified 12 genes that were associated with lymph node metastasis.[23] Hippo *et al.* identified several genes associated with lymph node metastasis, including Oct-2, and genes associated with the histological type, including liver-intestine cadherin.[24] These studies introduced a novel direction in which microarray analysis could be used to predict postoperative recurrences. Inoue *et al.* selected 78 genes that were differentially expressed between aggressive and non-aggressive cancers and constructed a prognostic scoring system.[25] Leung *et al.* found that high CCL18 expression levels were associated with prolonged overall and disease-free survival.[26] They also found that phospholipase A2 group IIA expression in gastric adenocarcinoma was associated with prolonged survival and less frequent metastasis.[27] Chen *et al.* demonstrated a survival prediction model consisting of three genes (*CD36*, *SLAM*, *PIM-1*) that was capable of predicting poor or good survival in 23 (76.7%) of 30 newly enrolled patients.[28] Most of these studies used surgical specimens to predict postsurgical survival and were conducted retrospectively. Thus, we think that our present prospective study is unique in that we used endoscopic biopsy samples to predict the survival time in patients with unresectable gastric cancer. In patients with unresectable cancer, endoscopic biopsy samples may be the most appropriate specimens available non-invasively for microarray analysis. Although tumor heterogeneity may pose problems when biopsy samples are used as representative tissue specimens and further investigation is required, we believe that endoscopic biopsy samples should continue to be used for microarray analyses. Current clinical study has been confronted with a number of obstacles. Microarray analysis for clinical studies, in particular, has been hampered with bottlenecks such as RNA quality, the extremely large number of genes to be analyzed, an immature analytical tool or methodology and so on. There are two types of obstacles: controllable obstacles and uncontrollable ones. One uncontrollable obstacle is a complex chemotherapy regimen. It is easy to say that a clinical biomarker study should be performed in one particular regimen. Chemotherapy regimen has, however, progressed and become more sophisticated in a short range of time. This study was prospective clinical study and was largely followed by a guideline, Recommendations for Tumor Marker Prognostic Studies (REMARK). To minimize

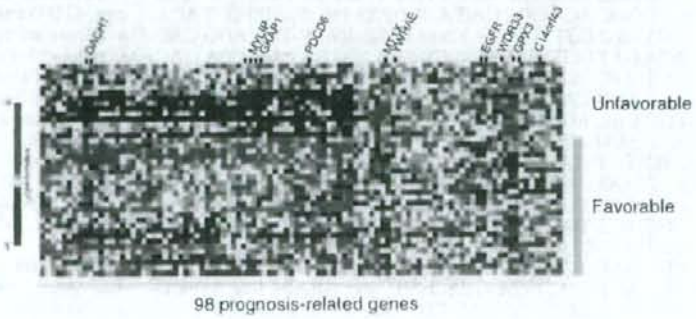

Fig. 1. Heat map of expression values for microarray identifying 98 genes whose expressions were correlated with survival. The hierarchical clustering of the 98 genes comparing the unfavorable prognosis group (survival time, <180 days) and favorable prognosis group (survival time, ≥180 days) is shown. The blue or red colors of each block represent the normalized gene expression levels. Each row represents a sample, and each column represents a gene. The 10 genes included in the multivariate analysis (Table 3) are shown.

Table 2. Prognosis-related genes identified using microarray analysis

P-value	Hazard ratio	Description	Gene	Probe set	Pass	PCR		
0.0002	1.8	Epidermal growth factor receptor	*EGFR*	201984_s_at	2	PCR	1	0.1
0.0005	0.1	DEAD (Asp-Glu-Ala-Asp) box polypeptide 54	*DDX54*	219111_s_at			2	0.1
0.0005	0.5	Chimerin (chimaerin) 2	*CHN2*	213385_at			3	0.1
0.0005	6.1	Ubiquitin-like domain containing CTD phosphatase 1	*UBLCP1*	227413_at			4	0.2
0.0006	0.5	PTK2 protein tyrosine kinase 2	*PTK2*	241387_at			5	0.2
0.0008	3.4	Der1-like domain family, member 2	*DERL2*	218333_at			6	0.2
0.0008	0.5	Leucine rich repeat containing 14	*LRRC14*	32062_at			7	0.2
0.0009	4.5	WD repeat domain 33	*WDR33*	222763_s_at		PCR	8	0.2
0.0009	0.1	Rhomboid domain containing 3	*RHBDD3*	217622_at			9	0.2
0.001	0.3	Myosin regulatory light chain interacting protein	*MYLIP*	228098_s_at	3	PCR	10	0.2
0.0013	4.7	Chromosome 14 open reading frame 43	*C14orf43*	225980_at		PCR	11	0.2
0.0013	0.2	BCL6 co-repressor	*BCOR*	223915_at			12	0.2
0.0013	0.5	MAD1 mitotic arrest deficient-like 1 (yeast)	*MAD1L1*	233921_s_at			13	0.2
0.0013	4.9	Chromosome 14 open reading frame 109	*C14orf109*	213246_at			14	0.2
0.0014	4.2	Hypothetical protein LOC124512	*LOC124512*	225808_at			15	0.2
0.0014	5.0	Ring finger protein 167	*RNF167*	212047_s_at			16	0.2
0.0014	0.6	Hypothetical LOC25845	*LOC25845*	225457_s_at			17	0.2
0.0014	4.2	General transcription factor II, i	*GTF2I*	232710_at			18	0.3
0.0014	0.2	Rho guanine nucleotide exchange factor (GEF) 10-like	*ARHGEF10L*	1570511_at			19	0.3
0.0014	0.3	G kinase anchoring protein 1	*GKAP1*	229312_s_at		PCR	20	0.3
0.0015	1.9	Glutathione peroxidase 3 (plasma)	*GPX3*	214091_s_at	2	PCR	21	0.3
0.0016	0.5	Dachshund homolog 1 (*Drosophila*)	*DACH1*	1567101_at	2	PCR	22	0.3
0.0016	0.3	Diacylglycerol kinase, theta 110kDa	*DGKQ*	226605_at			23	0.3
0.0017	0.6	Hepatocellular carcinoma-associated antigen 112	*HCA112*	218345_at			24	0.3
0.0018	3.5	Mediator of RNA polymerase II transcription, subunit 31 homolog	*MED31*	222867_s_at			25	0.3
0.0018	6.9	Tyrosine 3-monooxygenase/tryptophan 5-monooxygenase activation protein, epsilon polypeptide	*YWHAE*	210317_s_at		PCR	26	0.3
0.0018	0.1	KH domain containing, RNA binding, signal transduction associated 1	*KHDRBS1*	201488_x_at			27	0.3
0.0019	0.3	Solute carrier family 25 (mitochondrial carrier; Graves disease autoantigen), member 16	*SLC25A16*	210686_x_at			28	0.3
0.0019	4.9	Hypothetical protein LOC51255	*LOC51255*	223064_at			29	0.3
0.002	0.2	Cyclin L2 /// similar to Aurora kinase A-interacting protein	*CCNL2 /// LOC643556*	222999_s_at			30	0.3
0.002	7.4	Lectin, mannose-binding, 1	*LMAN1*	224629_at			31	0.3
0.002	0.2	Erythrocyte membrane protein band 4.1 like 4A	*EPB41L4A*	228259_s_at			32	0.3
0.0022	0.2	KIAA0999 protein	*KIAA0999*	204155_s_at			33	0.3
0.0022	0.5	ELOVL family member 7	*ELOVL7*	227180_at			34	0.3
0.0023	4.0	Churchill domain containing 1	*CHURC1*	233268_s_at			35	0.4
0.0024	4.0	Yippee-like 2 (*Drosophila*)	*YPEL2*	227020_at			36	0.4
0.0024	5.9	Hermansky–Pudlak syndrome 1	*HPS1*	210112_at			37	0.4
0.0025	0.3	Hypothetical protein LOC285831	*LOC285831*	228857_at			38	0.4
0.0026	3.5	CDC37 cell division cycle 37 homolog (*Saccharomyces cerevisiae*)-like 1	*CDC37L1*	219343_at			39	0.4
0.0026	2.1	Ankyrin repeat and SOCS box-containing 9	*ASB9*	205673_s_at			40	0.4
0.0026	0.2	Hypothetical gene supported by AK125149	*LOC401577*	239247_at			41	0.5
0.0026	0.3	TBC1 domain family, member 23	*TBC1D23*	236755_at			42	0.5
0.0026	0.3	MRNA full length insert cDNA clone EUROIMAGE 2362292		235505_s_at			43	0.5
0.0026	0.4	Dehydrogenase/reductase (SDR family) member 8	*DHRS8*	217989_at			44	0.5
0.0026	0.4	Nuclear receptor coactivator 2	*NCOA2*	242369_x_at			45	0.5
0.0026	0.2	MRNA; cDNA DKFZp667E0114 (from clone DKFZp667E0114)		235660_at			46	0.5
0.0027	0.4	Transforming, acidic coiled-coil containing protein 1	*TACC1*	242290_at			47	0.5
0.0027	0.2	POU domain, class 2, transcription factor 1	*POU2F1*	1562280_at			48	0.5
0.0027	2.9	p21(CDKN1A)-activated kinase 6	*PAK6*	1555310_a_at				0.5
0.0027	0.5	Mannosyl (alpha-1,3-)-glycoprotein β-1,4-N-acetylglucosaminyltransferase, isozyme A	*MGAT4A*	226039_at			50	0.5
0.0027	5.1	Zinc finger CCCH-type containing 14	*ZC3H14*	204216_s_at			51	0.5
0.0028	0.5	Acyl-CoA synthetase short-chain family member 2	*ACSS2*	235805_at			52	0.5
0.0028	0.3	Programmed cell death 6	*PDCD6*	222380_s_at		PCR	53	0.6
0.0029	3.8	ERGIC and golgi 2	*ERGIC2*	226422_at			54	0.6
0.0029	0.4	Erythrocyte membrane protein band 4.1 like 5	*EPB41L5*	225855_at			55	0.6
0.003	6.5	Chromosome 14 open reading frame 32	*C14orf32*	212644_s_at			56	0.6

doi: 10.1111/j.1349-7006.2008.00935.x

Table 2. *(Continued)*

P-value	Hazard ratio	Description	Gene	Probe set	Pass	PCR		
0.0031	0.2	Transcribed locus		239437_at			57	1.8
0.0031	0.3	DOT1-like, histone H3 methyltransferase (*S. cerevisiae*)	*DOT1L*	231297_at			58	1.9
0.0031	2.2	Transcription elongation factor A (SII)-like 8	*TCEAL8*	224819_at			59	1.9
0.0031	0.3	Laminin, β 1	*LAMB1*	236437_at			60	2.0
0.0032	2.7	FK506 binding protein 5	*FKBP5*	224840_at			61	2.0
0.0033	0.5	Integrin, α 6	*ITGA6*	244665_at			62	2.1
0.0034	2.7	COMM domain containing 9	*COMMD9*	218072_at			63	2.2
0.0034	0.2	Eukaryotic translation initiation factor 4 γ, 3	*EIF4G3*	201936_s_at			64	2.3
0.0035	0.5	235616_at	*235616_at*	235616_at			65	2.6
0.0036	1.9	Metallothionein 1X	*MT1X*	204326_x_at		PCR	66	2.6
0.0036	2.7	Peroxiredoxin 5	*PRDX5*	1560587_s_at			67	2.7
0.0037	0.3	Core-binding factor, runt domain, α subunit 2; translocated to, 2	*CBFA2T2*	207625_s_at			68	2.7
0.0037	0.4	Transcribed locus, moderately similar to XP_531878.2		230168_at			69	2.7
0.0038	0.3	Zinc finger protein 346	*ZNF346*	236267_at			70	2.8
0.0038	2.0	Metallothionein 1H-like protein /// hypothetical protein LOC650610	*LOC645745 /// LOC650610*	211456_x_at			71	2.9
0.0039	0.2	Hypothetical protein DKFZp586I1420	*DKFZp586I1420*	213546_at			72	3.4
0.0039	2.0	Adrenergic, β-2-, receptor, surface	*ADRB2*	206170_at			73	3.5
0.0039	0.3	CTD-binding SR-like protein rA9	*KIAA1542*	234952_s_at			74	3.5
0.0039	2.6	Peroxiredoxin 5	*PRDX5*	222994_at			75	3.6
0.004	0.2	ATPase, H^+ transporting, lysosomal 42kDa, V1 subunit C1	*ATP6V1C1*	226463_at			76	3.8
0.004	8.0	XK, Kell blood group complex subunit-related family, member 8	*XKR8*	218753_at			77	3.8
0.004	0.3	Caspase 6, apoptosis-related cystein peptidase	*CASP6*	242323_at			78	4.0
0.0041	0.4	Coagulation factor XII (Hageman factor)	*F12*	205774_at			79	4.0
0.0041	0.3	Centaurin, γ 2	*CENTG2*	240758_at			80	4.2
0.0042	0.6	LR8 protein	*LR8*	220532_s_at			81	4.2
0.0042	0.2	WD repeat domain 42A	*WDR42A*	243318_at			82	4.5
0.0042	2.6	Potassium channel tetramerisation domain containing 14	*KCTD14*	219545_at			83	4.7
0.0043	2.8	6-Phosphogluconolactonase	*PGLS*	218388_at			84	4.9
0.0044	3.8	Bruno-like 6, RNA binding protein (*Drosophila*)	*BRUNOL6*	227775_at			85	4.9
0.0044	2.3	Zinc finger protein 415	*ZNF415*	205514_at			86	5.0
0.0045	0.5	HIR histone cell cycle regulation defective homolog A (*S. cerevisiae*)	*HIRA*	240451_at			87	5.1
0.0046	0.5	Cardiolipin synthase 1	*CRLS1*	241741_at			88	5.9
0.0046	0.3	c-mer proto-oncogene tyrosine kinase	*MERTK*	233079_at			89	6.1
0.0047	0.2	Additional sex combs like 2 (*Drosophila*)	*ASXL2*	218659_at			90	6.5
0.0047	3.6	Platelet endothelial aggregation receptor 1	*PEAR1*	228618_at			91	6.9
0.0047	0.3	Core-binding factor, runt domain, α subunit 2; translocated to, 2	*CBFA2T2*	238549_at			92	7.4
0.005	0.6	Lysosomal associated protein transmembrane 4 β	*LAPTM4B*	208029_s_at			93	8.0

Pass, number of overlapped probes; PCR, the genes that were subsequently examined using real-time RT-PCR.

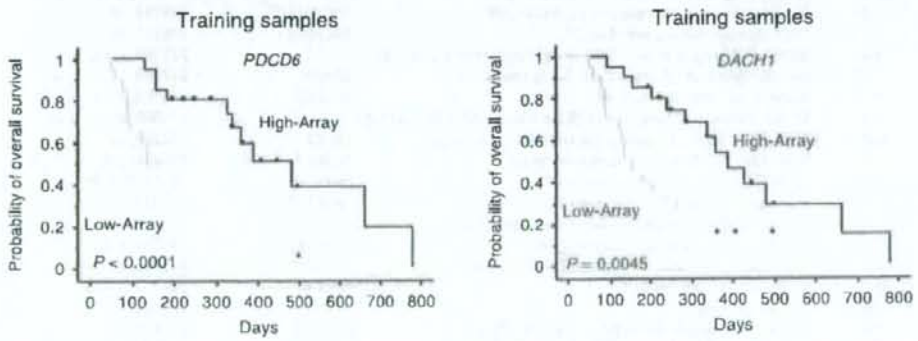

Fig. 2. Results of microarray data and patient survival in the training set of 40 patients. The Kaplan–Meier method was used for *DACH1* and *PDCD6*. The patients were divided into high and low expression groups by median values. The low *PDCD6* and *DACH1* expression groups had significantly poorer outcomes ($P < 0.0001$ and $P = 0.0045$). High-Array, group with high expression levels as determined by signal intensity of microarray data. Low-Array, group with low expression levels as determined by signal intensity of microarray data.

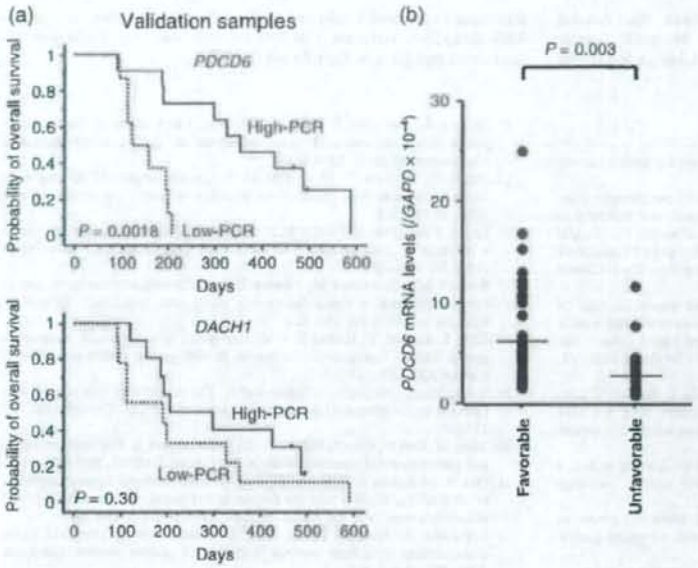

Fig. 3. Results of real-time reverse transcription polymerase chain reaction (RT-PCR) analysis and patient survival in the independent validation set of 19 samples. (a) The Kaplan–Meier method was used to estimate the overall survival. The low *PDCD6* expression groups had significantly poorer outcomes ($P = 0.0018$). High-PCR, group with high expression levels as determined by PCR. Low-PCR, group with low expression levels as determined by PCR. (b) All quantified expression levels of real time RT-PCR data are shown. The mRNA expressions of *PDCD6* were significantly lower in unfavorable group ($P = 0.003$) and varied ~25 fold (range, 0.98–25.1). Favorable, the patients with survival time over 180 days. Unfavorable, the patients with a survival time less than 180 days.

Table 3. Multivariate analysis of prognosis-related genes

Variable	Hazard ratio	95% confidence interval	*P*-value
Age (≥65)	1.78	0.570–5.559	0.3212
Sex (male)	3.26	0.732–14.489	0.1210
Performance status (≥1)	2.36	0.687–8.078	0.1728
Metastasis (≥3)	1.58	0.450–5.561	0.4739
Chemotherapy (5-FU)	1.48	0.402–5.475	0.5541
DACH1	0.38	0.175–0.817	0.0134
EGFR	1.41	0.992–2.001	0.0553
MT1X	0.71	0.317–1.600	0.4111
YWHAE	1.91	0.401–9.061	0.4169
GPX3	1.62	0.869–3.007	0.1293
PDCD6	0.06	0.010–0.334	0.0015
WDR33	1.38	0.268–7.067	0.7017
C14orf43	0.64	0.122–3.407	0.6045
MYLIP	0.67	0.221–2.042	0.4826
GKAP1	2.31	0.751–7.106	0.1440

Cox regression model was performed for multivariate analysis against each of the variables.

Table 4. Results of real-time *RT-PCR* for *PDCD6* and *DACH1* in an independent vallation set

Genes	Hazard ratio	95% confidence limits		*P*-value
		Upper	Lower	
*PDCD6**	0.29	0.12	0.71	0.007
DACH1	0.79	0.56	1.13	0.199

*, $P < 0.05$.

the uncontrollable factors, we aimed to avoid controllable factors with our best efforts. In this sense, we believe that the present study has succeeded in stratifying potential controllable variables.

Based on the results of the series of analyses conducted in the current study, we validated *PDCD6* as a molecular biomarker of the prognosis in gastric cancer.

PDCD6, also known as ALG-2 (apoptosis-linked gene-2), was first identified in a study on T-cell apoptosis conducted by Vito *et al.*[29] *PDCD6* encodes a calcium-binding protein that belongs to the penta-EF-hand protein family. The gene product participates in T-cell receptor-, Fas- and glucocorticoid-induced programmed cell death and cell proliferation. The stimulation of cells to enter the cell cycle is thought to drive the cellular apoptotic program, and the presence of additional survival or pro-apototic signals determines whether a cell proliferates or commits suicide. Krebs *et al.* indicated that the deregulation of such an obviously delicate balance could lead to pathological developments, such as cancer.[30] Detailed biological function of *PDCD6* genes in gastric cancer is still unclear. The speculated function may lead us to hypothesize that the expression is generally downregulated in cancer.

Our ultimate goal is to use real-time RT-PCR or immunohistochemical examination to identify patients with a poor prognosis prior to undertaking chemotherapy. We are now planning a large-scale prospective study based on the evidence obtained in the current study.

In conclusion, we identified prognostic biomarkers in patients with unresected gastric cancer, and our PCR-based single gene prediction strategy successfully predicted the overall survival of patients with gastric cancer. Our findings may provide a novel insight into the treatment of gastric cancer and may lead to a better understanding of this disease subgroup.

Acknowledgments

This work was supported by funds for the Third Term Comprehensive 10-Year Strategy for Cancer Control, a Grant-in-Aid for Scientific Research and the program for promotion of Fundamental Studies in Health Sciences of the National Institute of Biomedical Innovation (NiBio). The following people have played very important roles in the conduct of this project: Hiromi Orita, Hisanao Hamanaka, Ayumu Goto, Hisateru Yasui, Junichi Matsubara, Natsuko Okita, Takako Nakajima,

doi: 10.1111/j.1349-7006.2008.00935.x

Atsuo Takashima, Kei Muro, Takashi Ura, Hideko Morita, Mari Araake, Hisao Fukumoto, Tatsu Shimoyama, Naoki Hayama, Masayuki Takeda, Hideharu Kimura, Kazuko Sakai, Terufumi Kato and Jun-ya Fukai. We also thank Dr Richard Simon and Dr Amy Peng for providing us with the BRB ArrayTools software. This free software was very useful and has been developed for user-friendly applications.

References

1 Sastre J, Garcia-Saenz JA, Diaz-Rubio E. Chemotherapy for gastric cancer. *World J Gastroenterol* 2006; **12**: 204–13.
2 Vanhoefer U, Rougier P, Wilke H *et al.* Final results of a randomized phase III trial of sequential high-dose methotrexate, fluorouracil, and doxorubicin versus etoposide, leucovorin, and fluorouracil versus infusional fluorouracil and cisplatin in advanced gastric cancer: a trial of the European Organization for Research and Treatment of Cancer Gastrointestinal Tract Cancer Cooperative Group. *J Clin Oncol* 2000; **18**: 2648–57.
3 Ohtsu A, Shimada Y, Shirao K *et al.* Randomized phase III trial of fluorouracil alone versus fluorouracil plus cisplatin versus uracil and tegafur plus mitomycin in patients with unresectable, advanced gastric cancer: The Japan Clinical Oncology Group Study (JCOG9205). *J Clin Oncol* 2003; **21**: 54–9.
4 Sakata Y, Ohtsu A, Horikoshi N, Sugimachi K, Mitachi Y, Taguchi T. Late phase II study of novel oral fluoropyrimidine anticancer drug S-1 (1M tegafur-0.4M gimestat-1M otastat potassium) in advanced gastric cancer patients. *Eur J Cancer* 1998; **34**: 1775–20.
5 Koizumi W, Kurihara M, Nakano S, Hasegawa K. Phase II study of S-1, a novel derivative of 5-fluorouracil, in advanced gastric cancer. *Oncology* 2000; **58**: 191–7.
6 Shirao K, Shimada Y, Kondo H *et al.* Phase I–II study of irinotecan hydrochloride combined with cisplatin in patients with advanced gastric cancer. *J Clin Oncol* 1997; **15**: 921–7.
7 Boku N, Ohtsu A, Shimada Y *et al.* Phase II study of combination of irinotecan and cisplatin against metastatic gastric cancer. *J Clin Oncol* 1999; **17**: 319–23.
8 Boku N, Yamamoto S, Shirao K *et al.* Gastrointestinal Oncology Study Group/Japan Clinical Oncology Group. Randomized phase III study of 5-fluorouracil (5-FU) alone versus combination of irinotecan and cisplatin (CP) versus S-1 alone in advanced gastric cancer (JCOG9912) (Abstract). *Proc Am Soc Clin Oncol* 2007; **25**: 18S.
9 Chau I, Norman AR, Cunningham D, Waters JS, Oates J, Ross PJ. Multivariate prognostic factor analysis in locally advanced and metastatic esophago-gastric cancer – pooled analysis from three multicenter, randomized, controlled trials using individual patient data. *J Clin Oncol* 2004; **22**: 2395–403.
10 Metzger R, Leichman CG, Danenberg KD *et al.* ERCC1 mRNA levels complement thymidylate synthase mRNA levels in predicting response and survival for gastric cancer patients receiving combination cisplatin and 5-fluorouracil chemotherapy. *J Clin Oncol* 1998; **16**: 309–16.
11 Boku N, Chin K, Hosokawa K *et al.* Biological makers as a predictor for response and prognosis of unresectable gastric cancer patients treated with 5-fluorouracil and cis-platinum. *Clin Cancer Res* 1998; **4**: 1469–74.
12 Yonemura Y, Ninomiya I, Yamaguchi A *et al.* Evaluation of immunoreactivity for erbB-2 protein as a marker of poor short term prognosis in gastric cancer. *Cancer Res* 1991; **51**: 1034–8.
13 Sanz-Ortega J, Steinberg SM, Moro E *et al.* Comparative study of tumor angiogenesis and immunohistochemistry for p53, c-ErbB2, c-myc and EGFr as prognostic factors in gastric cancer. *Histol Histopathol* 2000; **15**: 455–62.
14 Shibata A, Parsonnet J, Longacre TA *et al.* CagA status of *Helicobacter pylori* infection and p53 gene mutations in gastric adenocarcinoma. *Carcinogenesis* 2002; **23**: 419–24.
15 Okusa Y, Ichikura T, Mochizuki H. Prognostic impact of stromal cell-derived urokinase-type plasminogen activator in gastric carcinoma. *Cancer* 1999; **85**: 1033–8.
16 Linder N, Haglund C, Lundin M *et al.* Decreased xanthine oxidoreductase is a predictor of poor prognosis in early-stage gastric cancer. *J Clin Pathol* 2006; **59**: 965–71.
17 Resnick MB, Gavilanez M, Newton E *et al.* Claudin expression in gastric adenocarcinomas: a tissue microarray study with prognostic correlation. *Hum Pathol* 2005; **36**: 886–92.
18 Kido S, Kitadai Y, Hattori N *et al.* Interleukin 8 and vascular endothelial growth factor – prognostic factors in human gastric carcinomas? *Eur J Cancer* 2001; **37**: 1482–7.
19 Xiangming C, Natsugoe S, Takao S *et al.* The cooperative role of p27 with cyclin E in the prognosis of advanced gastric carcinoma. *Cancer* 2000; **89**: 1214–9.
20 Yasui W, Oue N, Ono S, Mitani Y, Ito R, Nakayama H. Histone acetylation and gastrointestinal carcinogenesis. *Ann NY Acad Sci* 2003; **983**: 220–31.
21 Oue N, Motoshita J, Yokozaki H *et al.* Distinct promoter hypermethylation of p16INK4a, CDH1, and RAR-beta in intestinal, diffuse-adherent, and diffuse-scattered type gastric carcinomas. *J Pathol* 2002; **198**: 55–9.
22 Yamanaka R, Arao T, Yajima N *et al.* Identification of expressed genes characterizing long-term survival in malignant glioma patients. *Oncogene* 2006; **25**: 5994–6002.
23 Hasegawa S, Furukawa Y, Li M *et al.* Genome-wide analysis of gene expression in intestinal-type gastric cancers using a complementary DNA microarray representing 23 040 genes. *Cancer Res* 2002; **62**: 7012–17.
24 Hippo Y, Taniguchi H, Tsutsumi S *et al.* Global gene expression analysis of gastric cancer by oligonucleotide microarrays. *Cancer Res* 2002; **62**: 233–40.
25 Inoue H, Matsuyama A, Mimori K, Ueo H, Mori M. Prognostic score of gastric cancer determined by cDNA microarray. *Clin Cancer Res* 2002; **8**: 3475–9.
26 Leung SY, Yuen ST, Chu KM *et al.* Expression profiling identifies chemokine (C-C motif) ligand 18 as an independent prognostic indicator in gastric cancer. *Gastroenterology* 2004; **127**: 457–69.
27 Leung SY, Chen X, Chu KM *et al.* Phospholipase A2 group IIA expression in gastric adenocarcinoma is associated with prolonged survival and less frequent metastasis. *Proc Natl Acad Sci USA* 2002; **99**: 16203–8.
28 Chen CN, Lin JJ, Chen JJ *et al.* Gene expression profile predicts patient survival of gastric cancer after surgical resection. *J Clin Oncol* 2005; **23**: 7286–95.
29 Vito P, Lacana E, D'Adamio L. Interfering with apoptosis: Ca^{2+}-binding protein ALG-2 and Alzheimer's disease gene ALG-3. *Science* 1996; **271**: 521–5.
30 Krebs J, Saremaslani P, Caduff R. ALG-2: a Ca^{2+}-binding modulator protein involved in cell proliferation and in cell death. *Biochim Biophys Acta* 2002; **1600**: 68–73.

Med Oncol
DOI 10.1007/s12032-008-9127-2

ORIGINAL PAPER

Immunohistochemical expression of PTEN and phosphorylated Akt are not correlated with clinical outcome in breast cancer patients treated with trastuzumab-containing neo-adjuvant chemotherapy

Kan Yonemori · Koji Tsuta · Chikako Shimizu · Yutaka Hatanaka · Kaoru Hashizume · Makiko Ono · Tsutomu Kouno · Masashi Ando · Kenji Tamura · Noriyuki Katsumata · Tadashi Hasegawa · Takayuki Kinoshita · Yasuhiro Fujiwara

Received: 31 March 2008 / Accepted: 29 October 2008

Abstract The loss of PTEN and phosphorylated Akt (pAkt) expression is thought to be involved in the mechanism leading to trastuzumab resistance in patients with HER2-positive breast cancer. We retrospectively performed immunohistochemical analyses for estrogen receptor, progesterone receptor, HER2/neu, PTEN, pAkt, and p53 expression in tumor specimens obtained before and after trastuzumab-containing neo-adjuvant chemotherapy. The intensity of staining was evaluated for each biomarker, and the correlations between the immunohistochemical profiles and the clinical outcome were analyzed. The changes in the immunohistochemical profiles between specimens obtained before and after trastuzumab-containing neo-adjuvant chemotherapy were evaluated for patients with residual tumors. The present study included 44 patients with breast cancer who received trastuzumab-containing neo-adjuvant chemotherapy. Seventeen patients achieved a pathological complete response. The patients were positive for PTEN and pAkt (PTEN = 14%, $N = 6/44$; pAkt, 80%, $N = 35/44$). The expression of both PTEN and pAkt were not correlated with pathological complete response. Persistent HER2/neu over-expression after neo-adjuvant chemotherapy was significantly associated with recurrence. Among 27 patients with residual cancer, the percentages of patients with HER2/neu-positive or pAkt-positive tumors were low, but PTEN expression was elevated. The present study suggested that neither the immunohistochemical expression of PTEN nor the expression of pAkt was associated with the clinical outcome of trastuzumab-containing neo-adjuvant chemotherapy. Except among patients with pathological complete remission, the persistent over-expression of HER2/neu may be a poor prognostic factor.

Keywords Breast cancer · Neoadjuvant chemotherapy · pAkt · PTEN · Trastuzumab

K. Yonemori (✉) · C. Shimizu · M. Ono · T. Kouno · M. Ando · K. Tamura · N. Katsumata · Y. Fujiwara
Breast and Medical Oncology Division, National Cancer Center Hospital, 5-1-1 Tsukiji, Chuo-ku, Tokyo 104-0045, Japan
e-mail: kyonemor@ncc.go.jp; yonemori-kan@pmda.go.jp

K. Tsuta · Y. Fujiwara
Clinical Laboratory Division, National Cancer Center Hospital, 5-1-1 Tsukiji, Chuo-ku, Tokyo 104-0045, Japan

Y. Hatanaka · K. Hashizume
Medical Science Division, Dako Japan, Inc, 2-5-1, Kouraku, Bunkyo-ku, Tokyo 112-0004, Japan

T. Hasegawa
Department of Surgical Pathology, Sapporo Medical School of Medicine, South 1 West 16, Chuo-ku, Sapporo, Hokkaido 060-8543, Japan

T. Kinoshita
Breast Surgery Division, National Cancer Center Hospital, 5-1-1 Tsukiji, Chuo-ku, Tokyo 104-0045, Japan

Introduction

Breast cancer remains the major cause of death from cancer among woman throughout the world. Most breast cancers are thought to be systemic diseases at the time of diagnosis, and recurrence as a result of sub-clinical micro-metastasis is common. Recent advances in multidisciplinary approaches for treating breast cancer, including both neo-adjuvant chemotherapy and adjuvant chemotherapy, have played important roles in improving the survival rate [1]. A previous study revealed that patients who achieved a pathological complete response (pCR) had longer relapse-free survival periods than patients without pCR after neo-adjuvant

Published online: 18 November 2008

chemotherapy [2]. This study suggested that the chem otherapeutic response at the primary lesion may be correlated with the chemotherapeutic response of micrometastases; therefore, the selection of a chemotherapeutic regimen that best enables pCR may improve both the relapse-free and overall survival rates.

The epidermal growth factor receptor/HER family is involved in cell proliferation, differentiation, and survival. HER2/neu over-expression and *HER2/neu* amplification are widely known markers of aggressive tumor behavior, and a poor clinical outcome in breast cancer patients are observed in approximately 20–30% of breast cancer patients [3]. Trastuzumab, a monoclonal antibody against HER2/neu, has been shown to have a significant efficacy in both adjuvant and metastatic settings [4, 5]. Recently, a randomized phase II trial revealed that trastuzumab-containing neo-adjuvant chemotherapy significantly improved the pCR rate, compared with neo-adjuvant chemotherapy alone, in patients with HER2/neu-positive breast cancer [6].

Immunohistochemistry and fluorescence in situ hybridization (FISH) are currently available methods for identifying patients who are likely to benefit from trastuzumab; however, trastuzumab is ineffective in some patients and progression may still occur. Currently, the possible mechanisms of trastuzumab-resistance include the down-regulation of p27; the activation of insulin-like growth factor receptor (IGF-1R); the loss of expression of PTEN, pAkt, or the interaction HER receptor family; the masking of HER2/neu by membrane-associated glycoprotein mucin-4; angiogenesis; or antibody-dependent cellular toxicity [7]. These hypotheses remain controversial, and some studies that have assessed IGF-1R and p53 levels in clinical samples have reported negative results [8, 9].

PTEN is a dual phosphatase that mainly dephosphorylates position D3 of membrane phosphatidylinositol-3, 4, 5 triphosphate (PI3, 4, 5P3) and is a negative regulator of pAkt. Recently, Nagata et al. suggested that PTEN activation contributes to trastuzumab-induced tumor inhibition and that the loss of PTEN predicts trastuzumab resistance in patients with breast cancer [10]. The authors also validated their hypothesis in 47 metastatic breast cancer patients treated with a taxane-plus-trastuzumab therapy, revealing a statistically significant difference in the clinical response [10]. To test this hypothesis in patients with HER2-positive primary breast cancer, we compared the relationship between clinical outcome and the expression of immunohistochemical profiles, including those of p53, hormone receptors, PTEN, and pAkt, in patients receiving trastuzumab-containing neo-adjuvant chemotherapy. In addition, we investigated the changes in these profiles using specimens obtained before and after trastuzumab-containing neo-adjuvant chemotherapy.

Patients and methods

Patients

A total of 229 patients with breast cancer were treated with neo-adjuvant chemotherapy between January 1999 and January 2006 at the National Cancer Center Hospital. There were 49 patients who were classified as having HER2/neu-positive breast cancer (HER2/neu 3+ or HER2/neu 2+ and FISH-positive) and who received trastuzumab-containing neo-adjuvant chemotherapy. Of these, we identified 44 patients with adequate tumor tissue samples available for retrospective research. Trastuzumab was administered initially using an intravenous loading dose of 4 mg/kg, followed by weekly infusions of trastuzumab (2 mg/kg) in combination with weekly paclitaxel therapy. The dosages of the neo-adjuvant chemotherapy regimens were followed as: CEF therapy (cyclophosfamide, 500 mg/m^2, i.v. on day 1; epirubicin, 100 mg/m^2, i.v. on day 1; 5FU, 500 mg/m^2, i.v. on day 1; 21-day cycles), AC therapy (doxorubicin, 60 mg/m^2, i.v. on day 1; cyclophosphamide, 600 mg/m^2, i.v. on day 1; 21-day cycles), AT therapy (doxorubicin, 50 mg/m^2, i.v. on day 1; docetaxel, 60 mg/m^2, i.v. on day 1; 21-day cycles), and weekly paclitaxel therapy (80 mg/m^2, i.v. on day 1; 7-day cycles).

Tissue samples and microscopic and immunohistochemical analysis

Tissue samples were obtained from core-needle biopsy specimens before neo-adjuvant chemotherapy and from surgical specimens (mastectomy or lumpectomy) after neo-adjuvant chemotherapy. All hematoxylin-eosin stained core-needle biopsy specimens were reviewed by a pathologist (K. T.), and tissue sample were confirmed to contain adequate amounts of cancer tissue for use in the present study.

After surgical treatment, the pathologist evaluated the pathological responses of all the specimens using hematoxylin-eosin staining slides. pCR was defined as the complete disappearance of invasive cancer cells in the primary tumor and the axilla. We also evaluated the immunohistochemical changes in biomarker expression in the 27 patients who did not achieve pCR.

The pathological and immunohistochemical examinations were conducted by the same pathologists (K. T. and K. S.), who were blinded to the clinical statuses of the patients. Formalin-fixed, paraffin-embedded tissue samples were sectioned 4-μm thick and mounted on charged slides. Immunochistochemical staining of p53 (clone DO7; Dako, Glostrup, Denmark), ER (clone 1D5; Dako), and PgR (clone PgR636; Dako), were performed using the streptoavidin–biotin method, and were considered to be positive if

10% or more of the nuclei in the invasive component of the tumor was stained [8, 11]. The HER2/neu status, as assessed using Herceptest (Dako), was scored on a scale of 0–3+, according to the Dako scoring system. Clone 6H2.1 (Dako) and clone 14-5 (Dako) were used for immunohistochemical staining of PTEN and pAkt, respectively. For PTEN and pAkt, the slides were pretreated using heat-induced epitope retrieval and target retrieval solution, pH 9.0 (S2368; Dako), at 95–99°C for 40 min and then cooled for 20 min at room temperature. Immunohistochemistry was performed using the specified detection systems (ChemMate; Dako). Finally, the slides were incubated in DAB + substrate/chromogen solution (K3468; Dako) for 10 min, rinsed in diluted water, counterstained with hematoxylin, and mounted. Negative controls, in which the primary antibody was omitted, were also included in each run. Primary lung cancers and the stroma of endometria with a strong staining pattern (3+) were used as positive controls for PTEN, while primary lung cancer with a strong staining pattern (3+) was used as a positive control for pAkt in each run. The positive staining for PTEN was defined as cytoplasmic staining, which was same as internal control such as peripheral nerve. Positive staining for pAkt was defined as distinct cytoplasmic staining, which was recognized by low power fields. We defined cases with a score of 0 as being negative for PTEN and pAKT in the statistical analysis.

Statistical analysis

The Kaplan–Meier method was used to estimate the recurrence-free survival and the overall survival. Recurrence-free survival was measured from the first day of treatment until recurrence or the final day of the follow-up period without recurrence; Overall survival was measured from the first day of treatment until death or the final day of the follow-up period. The relationships between the expression of the biomarkers (p53, estrogen receptor, progesterone receptor, HER2/neu, PTEN, and pAkt), and the clinical outcomes of the patients were compared using the Chi-square test, the Fisher-exact test, and the log-rank test. All the statistical analyses were performed using SPSS 12.0J (SPSS Inc., Chicago, IL, USA), and the significance level for the results was set at 0.05 (two-sided).

Results

The present study included 44 patients. The patient's clinical characteristics are summarized in Table 1. Eighteen patients received CEF therapy followed by weekly paclitaxel/trastuzumab therapy, 11 patients received AC therapy followed by weekly paclitaxel/trastuzumab therapy, 8 patients received AT therapy followed by weekly paclitaxel/trastuzuab therapy, and 7 patients received weekly paclitaxel/trastuzumab therapy. None of the patients had progressive disease during neo-adjuvant chemotherapy. The median time between the last administration of neo-adjuvant chemotherapy until surgery was 5 weeks. Among 28 patients who had undergone a mastectomy, 9 patients received adjuvant radiotherapy. Sixteen patients received breast-conserving surgery followed by adjuvant radiotherapy. Nine patients received adjuvant hormone therapy.

Table 1 Patient characteristics

Characteristics	Value
Median age (range)	57 (33–78)
Side (right/left)	21/23
Median ECOG performance status	0
Menopausal status	
Pre-menopause	15 (34%)
Post-menopause	29 (66%)
Median clinical tumor size (range)	50 mm (20–120)
Number of patients with clinical lymph node swelling	23 (52%)
UICC-TNM staging	
IIA	15 (34%)
IIB	13 (30%)
IIIA	10 (23%)
IIIB	6 (13%)

After primary treatment, 12 patients developed recurrent disease: 3 loco-regional recurrences and 9 systemic recurrences. The sites of first relapse included six lung metastases, five liver metastases, three brain metastases, three loco-regional metastases, one bone metastasis, and one lymph node metastasis. Five patients died as a result of disease progression. The 5-year survival rate was 84%, and the 5-year recurrence-free survival rate was 65%.

Of the 44 patients, 17 patients achieved pCR. The median pathological tumor size of the patients with non-pCR was 15 mm (range, 0–100 mm). Significant differences in recurrence-free survival but overall survival were seen between patients with or without pCR (log-rank test, $P = 0.016$, 5-year recurrence-free survival rate; 86% vs. 52%, $p = 0.086$, 5-year survival rate; 100% vs. 77%, respectively). The relationship between pCR and the results of immunohistochemical staining of the biomarkers before neo-adjuvant chemotherapy are summarized in Table 2. None of the biomarkers examined in the specimens obtained at the time of diagnosis were significantly associated with either pCR or recurrence (Chi-square test, Fisher-exact test, $P > 0.1$).

Table 2 Relationship between pCR and immunohistochemical profiles in specimens at the time of diagnosis (Chi-square test and Fisher-exact test)

Variables	Total (%) $n = 44$	pCR		*P*-value
		pCR ($n = 17$)	Non-pCR ($n = 27$)	
Grade[a]				0.99
1	4 (9)	1	3	
2–3	40 (91)	16	24	
p53				0.680
Negative	25 (57)	9	16	
Positive	19 (43)	8	11	
ER				0.065
Negative	39 (89)	13	26	
Positive	5 (11)	4	1	
PgR				0.273
Negative	41 (93)	17	24	
Positive	3 (7)	0	3	
ER and/or PgR				0.402
Negative	37 (85)	13	24	
Positive	7 (15)	4	3	
PTEN				0.186
Negative	38 (86)	13	25	
Positive	6 (14)	4	2	
pAkt				0.275
Negative	9 (20)	5	4	
Positive	35 (80)	12	23	

Abbreviations: *pCR* pathological complete response

[a] Grade was defined using hematoxylin-eosin staining

Table 3 Relationship between recurrence and immunohistochemical profiles in residual tumor specimens obtained after neoadjuvant chemotherapy (Chi-square test and Fisher exact test)

Variables	Recurrence		*P*-value
	Rec[b] ($n = 11$)	Non-rec ($n = 16$)	
Grade[a]			0.618
1	1	4	
2–3	10	12	
p53			0.411
Negative	6	12	
Positive	5	4	
ER			0.99
Negative	10	14	
Positive	1	2	
PgR			0.99
Negative	11	15	
Positive	0	1	
ER and/or PgR			0.624
Negative	10	13	
Positive	1	3	
HER2/neu			0.008
Negative	0	8	
Positive	11	8	
PTEN			0.391
Negative	7	13	
Positive	4	3	
pAkt			0.453
Negative	5	5	
Positive	6	11	

Abbreviations: *Rec* recurrence

[a] Grade was defined using hematoxylin-eosin staining

[b] Twelve patients had recurrences in the present study. One patient with pCR was excluded in this statistical analysis

The relationship between recurrence and the results of immunohistochemical staining in the surgical specimens obtained after neo-adjuvant chemotherapy are summarized in Table 3. Only a persistent HER2/neu-positive status in the surgical specimens obtained after neo-adjuvant chemotherapy was significantly associated with recurrence (Fisher-exact test, $P = 0.008$), and the expressions of the other biomarkers were not associated with recurrence.

The proportions of changes in the immunohistochemical profiles before and after neo-adjuvant chemotherapy are summarized in Fig. 1. The changes in the immunohistochemical profiles were not correlated with clinical outcome (data not shown).

Discussion

This study demonstrated that clinical outcome, including pCR, recurrence, was not correlated with the immunohistochemical profiles of p53, estrogen receptor, progesterone receptor, PTEN, or pAkt in specimens obtained before trastuzumab-containing neo-adjuvant chemotherapy.

Interestingly, there were 38 patients with negative PTEN expression and 13 patients who achieved a pCR in the present study. Although we had hypothesized that the loss of PTEN and pAkt expression would influence the clinical outcome of trastuzumab-containing therapy, such as the rate of pCR, the results of the present study did not support our hypothesis, which had been based on the results of Nagata et al's study [10]. One explanation for this contradiction is that the neo-adjuvant chemotherapy used in the present study contained cytotoxic agents plus trastuzumab. HER2/neu over-expression is reportedly associated with sensitivity to anthracycline-containing chemotherapy [12]. Therefore, cytotoxic neo-adjuvant chemotherapy including anthracycline may be a confounding factor in evaluations of the impact of the loss of PTEN. There are also multiple

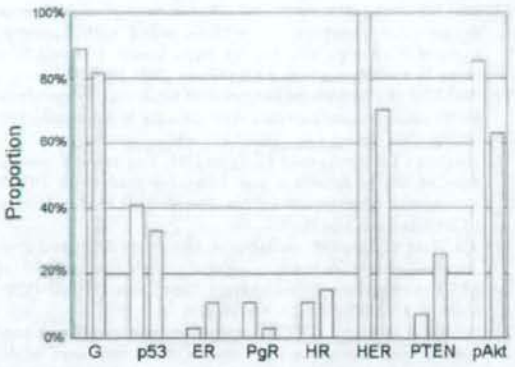

Fig. 1 Proportions of changes in the immunohistochemical profiles of specimens obtained before and after neo-adjuvant chemotherapy in patients with non-pCR ($n = 27$). Abbreviations: G, grade; HR, hormone receptor positive for ER and/or PgR; HER, HER2/neu

hypotheses regarding the mechanism(s) of primary or acquired resistance to trastuzumab [13]. Thus, the mechanism of trastuzumab-resistance may be difficult to explain using only one hypothesis.

The limitations of this study included the small sample size and the considerable heterogeneity in the chemotherapy treatment regimens. However, the majority of the patients had received chemotherapy that had included both an anthracycline and a taxane, and the treatment outcome among the patients was considered representative.

More essentially, the negative results might be attributable to the antibodies used for PTEN and pAkt detection or to a technical problem related to the immunohistochemistry studies. The loss of PTEN and pAkt expression has been reported to occur at various frequencies, [14–16] and the high frequency of the loss of PTEN and pAkt expression observed in the present study was the same as that in previous studies [14, 16]. The monoclonal antibody used in this study, 6H2.1, has been reported to be the only antibody correlated with the presence of molecular alterations in PTEN and to be associated significantly with immunostaining for pAkt; thus, we considered 6H2.1 to be the most suitable antibody for detecting the inactivation of PTEN, compared with the three other known antibodies [17]. In addition, 6H2.1 has been shown to have the same reactivity as the antibody that was used to analyze the loss of PTEN expression in a previous study by Nagata et al [10]. The immunohistochemical staining experiments in the present study were prudentially performed using both positive and negative controls, according to the methods described in a previous study [18], and we believe that any technical problems that may have occurred were of a limited nature.

Another recent study has described a patient cohort that received single-agent trastuzumab in a neo-adjuvant setting; in this previous study, no relationship between tumor response and pAkt expression was reported [19]. Although the different definition of response among patients with operable breast cancer and those with metastatic disease, that is clinical tumor regression and pathological eradication of the tumor, may be one possible explanation for the conflicting results among the studies. At any rate, it is difficult to make any conclusions regarding the role of the loss of PTEN and pAkt expression based on these limited data sets [14, 19], and the exploration of the PI3 K signaling pathway may not lead to a simple breakthrough in our understanding of trastuzumab resistance.

Although changes in the immunohistochemical profiles were frequently observed, such changes may not be useful for predicting clinical outcome. A previous study reported that neo-adjuvant chemotherapy had a minor, but significant (8%), effect on hormone status [20]. However, the HER2/neu status reportedly remained unchanged after neo-adjuvant chemotherapy; thus, HER2/neu expression was regarded as a stable phenotype [20, 21]. Conversely, other studies have reported that the HER2/neu status changed in 15–25% of patients, and the hormone receptor status changed in 26–42% of patients, after neo-adjuvant chemotherapy [22, 23]. Most HER2/neu status changes tend to represent down-regulation [23]. The frequency of changes in immunohistochemical profiles and their influences on clinical outcome are still controversial in neo-adjuvant chemotherapy settings. In addition, these studies included only patients treated without trastuzumab, so the influence of trastuzumab on HER2/neu expression is uncertain. The results of the present study suggest that the HER2/neu status may be altered and down-regulated by the addition of trastuzumab therapy to neo-adjuvant chemotherapy. Further studies on the effects of treatment on immunohistochemical profile changes, tumor cell biology, and/or trastuzumab resistance are needed.

In present study, persistent HER2/neu over-expression in the surgical specimen after trastuzumab-containing neo-adjuvant chemotherapy was associated with recurrence in patients without pCR; this observation may hold a clue to solving the mechanism of resistance to trastuzumab therapy. Previous studies have demonstrated that the down-regulation of target molecules, as shown by immunohistochemical staining in specimens obtained before and after neo-adjuvant chemotherapy, was significantly associated with both the tumor response and RFS, while persistent expression was associated with relapse [24, 25]. In addition, a recent study revealed that a short period of administration, such as 3 weeks of trastuzumab therapy, did not lead to the down-regulation of HER2/neu and did not result in any changes in expression level [19]. Concerning these results, the cancer cells with persistent HER2/neu over-expression after 3 months of trastuzumab treatment may be truly resistant to trastuzumab.

In the coming era of molecular-targeted drugs, multiple options of targeted therapy is becoming an increasingly important problem [7, 13]. However, the selection of appropriate candidates for trastuzumab therapy, which has now become a "classic" targeted therapy, still requires more investigation.

Acknowledgments This study was supported by grants from the Ministry of Health, Labour, and Welfare. The authors thank Miwa Yoshida, Tadahiko Shien, Takashi Hojo, Sadako Tanaka-Akashi (Breast Surgery Division, National Cancer Center Hospital), Eriko Nakano, Mayu Yunokawa, (Breast and Medical Oncology Division, National Cancer Center Hospital), and Kunihiko Seki (Pathology Division, JR Tokyo Hospital) for their assistance.

References

1. Mauri D, Pavlidis N, Ioannidis JP. Neoadjuvant versus adjuvant systemic treatment in breast cancer: a meta-analysis. J Natl Cancer Inst. 2005;97:188–94.
2. Fisher B, et al. Effect of preoperative chemotherapy on the outcome of woman with operable breast cancer. J Clin Oncol. 1996; 16:2672–85.
3. Slamon DJ, et al. Human breast cancer: correlation of relapse and survival with amplification of HER2/neu oncogene. Science. 1987;235:177–82. doi:10.1126/science.3798106.
4. Slamon DJ, et al. Use of chemotherapy plus a monoclonal antibody against HER2 for metastatic breast cancer that overexpresses HER2. N Engl J Med. 2001;344:783–92. doi:10.1056/NEJM200103153441101.
5. Piccart-Gebhart MJ, et al. Trastuzumab after adjuvant chemotherapy in HER2-positive breast cancer. N Engl J Med. 2005;353: 1659–72. doi:10.1056/NEJMoa052306.
6. Buzdar AU, et al. Significantly higher pathologic complete remission rate after neoadjuvant therapy with trastuzumab, paclitaxel, and epirubicin chemotherapy: results of a randomized trial in human epidermal growth factor receptor 2-positive operable breast cancer. J Clin Oncol. 2005;23:3676–85. doi:10.1200/JCO.2005.07.032.
7. Nahta R, Yu D, Hung MC, Hortobagyi GN, Esteva FJ. Mechanisms of disease: understanding resistance to HER2-tageted therapy in human breast cancer. Nat Clin Pract Oncol. 2006;3: 269–80. doi:10.1038/ncponc0509.
8. Kostler WJ, et al. The efficacy of trastuzumab in Her-2/neu-overexpressing metastatic breast cancer is independent of p53 status. J Cancer Res Clin Oncol. 2005;131:420–8. doi:10.1007/s00432-005-0670-3.
9. Kostler WJ, et al. Insulin-like growth factor-1 receptor expression does not predict for resistance to trastuzumab-based treatment in patients with HER2/neu over-expressing metastatic breast cancer. J Cancer Res Clin Oncol. 2006;132:9–18. doi:10.1007/s00432-005-0038-8.
10. Nagata Y, et al. PTEN activation contributes to tumor inhibition by trastuzumab, and loss of PTEN predicts trastuzumab resistance in patients. Cancer cell. 2004;6:117–27. doi:10.1016/j.ccr.2004.06.022.
11. Ellis MJ, et al. Letrozole is more effective neoadjuvant endocrine therapy than tamoxifen for erbB-1- and/or erbB-2-positive, estrogen receptor-positive primary breast cancer: evidence from phase III randomized trial. J Clin Oncol. 2001;19:3808–16.
12. Petit T, et al. Chemotherapy response of breast cancer depends on HER2 status and anthracycline dose intensity in the neoadjuvant setting. Clin Cancer Res. 2001;7:1577–81.
13. Valabrega G, Montemurro F, Aglietta M. Trastuzumab: mechanism of action, resistance and future perspectives in HER2-overexpressing breast cancer. Ann Oncol. 2007;18:977–84. doi: 10.1093/annonc/mdl475.
14. Xia W, et al. Lapatinib antitumor activity is not dependent upon phosphate tensin homologue deleted on chromosome 10 in erbB2-overexpressing breast cancers. Cancer Res. 2007;67:1170–5. doi:10.1158/0008-5472.CAN-06-2101.
15. Lee JS, et al. Reduced PTEN expression is associated with poor outcome and angiogenesis in invasive ductal carcinoma of the breast. Appl Immunohistochem Mol Morphol. 2004;12:205–10. doi:10.1097/00129039-200409000-00004.
16. Tokunaga E, et al. Akt is frequently activated in HER2/neu-positive breast cancer and associated with poor prognosis among hormone-treated patients. Int J Cancer. 2006;118:284–9. doi: 10.1002/ijc.21358.
17. Pallares J, et al. Immunohistochemical analysis of PTEN in endometrial carcinoma: a tissue microarray study with a comparison of four commercial antibodies in correlation with molecular abnormalities. Mod Pathol. 2004;18:1–9.
18. Mutter GL, Lin MC, Fitzgerald JT, Kum JB, Eng C. Changes in endometrial PTEN expression throughout the human menstrual cycle. J Clin Endocrinol Metab. 2000;85:2334–8. doi:10.1210/jc.85.6.2334.
19. Mohsin SK, et al. Neoadjuvant trastuzumab induces apotosis in primary breast cancers. J Clin Oncol. 2005;23:2460–8. doi:10.1200/JCO.2005.00.661.
20. Burcombe RJ, et al. Evaluation of ER, PgR, HER2 and Ki-67 as predictors of response to neoadjuvant anthracycline chemotherapy for operable breast cancer. Br J Cancer. 2005;92:147–55. doi: 10.1038/sj.bjc.6602256.
21. Taucher S, et al. Influence of neoadjuvant therapy with epirubicin and docetaxel on the expression of HER2/neu in patients with breast cancer. Breast Cancer Res Treat. 2003;82:207–13. doi: 10.1023/B:BREA.0000004378.15859.51.
22. Piper GL, Patel NA, Patel JA, Malay MB, Julian TB. Neoadjuvant chemotherapy for locally advanced breast cancer results in alterations in preoperative tumor marker status. Am Surg. 2004; 70:1103–6.
23. Neubauer H, et al. Changes in tumor biological markers during primary systemic chemotherapy. Anticancer Res. 2008;28: 1797–804.
24. Arpino G, et al. Predictive value of apoptosis proliferation, HER2, and topoisomerase IIa for anthracycline chemotherapy in locally advanced breast cancer. Breast Cancer Res Treat. 2005;92:69–75. doi:10.1007/s10549-005-1721-9.
25. Tinari N, et al. Changes of topoisomerase IIa expression in breast tumors after neoadjuvant chemotherapy predicts relapse-free survival. Clin Cancer Res. 2006;12:1501–6. doi:10.1158/1078-0432.CCR-05-0978.

Cancer Chemother Pharmacol (2008) 62:529–537
DOI 10.1007/s00280-007-0634-1

ORIGINAL ARTICLE

Impact of *CYP3A4* haplotypes on irinotecan pharmacokinetics in Japanese cancer patients

Kimie Sai · Yoshiro Saito · Hiromi Fukushima-Uesaka · Koichi Kurose · Nahoko Kaniwa · Naoyuki Kamatani · Kuniaki Shirao · Noboru Yamamoto · Tetsuya Hamaguchi · Hideo Kunitoh · Yuichiro Ohe · Tomohide Tamura · Yasuhide Yamada · Hironobu Minami · Atsushi Ohtsu · Teruhiko Yoshida · Nagahiro Saijo · Jun-ichi Sawada

Received: 6 July 2007 / Accepted: 22 October 2007 / Published online: 8 November 2007

Abstract
Background and purpose Cytochrome P450 3A4 (CYP3A4) converts an anticancer prodrug, irinotecan, to inactive metabolites such as APC. However, the contribution of *CYP3A4* genetic polymorphisms to irinotecan pharmacokinetics (PK) and pharmacodynamics (PD) is not fully elucidated. In paclitaxel-administered cancer patients, an association of *CYP3A4*16B* harboring the low activity allele **16* [554C > G (Thr185Ser)] has been shown with altered metabolite/paclitaxel area under the plasma concentration–time curve (AUC) ratios, suggesting a possible impact of **16B* on the PK of other drugs. In this study, the effects of *CYP3A4* haplotypes including **16B* on irinotecan PK/PD were investigated in irinotecan-administered patients.
Methods The *CYP3A4* genotypes for 177 Japanese cancer patients who received irinotecan were defined in terms of

K. Sai (✉)
Division of Biosignaling, National Institute of Health Sciences,
1-18-1 Kamiyoga, Setagaya-ku, Tokyo 158-8501, Japan
e-mail: sai@nihs.go.jp

Y. Saito · J.-i. Sawada
Division of Biochemistry and Immunochemistry,
National Institute of Health Sciences,
1-18-1 Kamiyoga, Setagaya-ku, Tokyo 158-8501, Japan

H. Fukushima-Uesaka
Project Team for Pharmacogenetics, National Institute of Health Sciences, 1-18-1 Kamiyoga, Setagaya-ku, Tokyo 158-8501, Japan

K. Kurose · N. Kaniwa
Division of Medical Safety Science,
National Institute of Health Sciences,
1-18-1 Kamiyoga, Setagaya-ku, Tokyo 158-8501, Japan

N. Kamatani
Division of Genomic Medicine,
Department of Advanced Biomedical Engineering and Science,
Tokyo Women's Medical University,
8-1 Kawada-cho, Shinjuku-ku, Tokyo 162-8666, Japan

K. Shirao · N. Yamamoto · T. Hamaguchi · H. Kunitoh ·
Y. Ohe · T. Tamura · Y. Yamada
Division of Internal Medicine,
National Cancer Center Hospital,
5-1-5 Tsukiji, Chuo-ku, Tokyo 104-0045, Japan

Present Address:
K. Shirao
Department of Medical Oncology,
Oita University Faculty of Medicine,
1-1 Idaigaoka, Hasama-machi, Yufu 879-5593, Japan

H. Minami
Division of Oncology/Hematology,
National Cancer Center Hospital East,
6-5-1 Kashiwanoha, Kashiwa, Chiba 277-8577, Japan

Present Address:
H. Minami
Medical Oncology, Department of Medicine,
Kobe University Hospital and Graduate School of Medicine,
7-5-2 Kusunoki-cho, Chuo-ku, Kobe 650-0017, Japan

A. Ohtsu
Division of Gastrointestinal Oncology/Digestive Endoscopy,
National Cancer Center Hospital East,
6-5-1 Kashiwanoha, Kashiwa, Chiba 277-8577, Japan

T. Yoshida
Genetics Division, National Cancer Center Research Institute,
5-1-5 Tsukiji, Chuo-ku, Tokyo 104-0045, Japan

N. Saijo
National Cancer Center Hospital East,
6-5-1 Kashiwanoha, Kashiwa, Chiba 277-8577, Japan